CONFIDENTIAL

Copy 4
RM L58A31

NACA RM L58A31

RESEARCH MEMORANDUM

EFFECTS OF SHOCK—BOUNDARY-LAYER INTERACTION ON THE PERFORMANCE OF A LONG AND A SHORT SUBSONIC ANNULAR DIFFUSER

By Charles C. Wood and John R. Henry

Langley Aeronautical Laboratory
Langley Field, Va.

UNCLASSIFIED

CLASSIFIED DOCUMENT

This material contains information affecting the National Defense of the United States within the meaning of the espionage laws, Title 18, U.S.C., Secs. 793 and 794, the transmission or revelation of which in any manner to an unauthorized person is prohibited by law.

NATIONAL ADVISORY COMMITTEE
FOR AERONAUTICS

WASHINGTON

April 15, 1958

CONFIDENTIAL

NACA RM L58A31

NATIONAL ADVISORY COMMITTEE FOR AERONAUTICS

RESEARCH MEMORANDUM

EFFECTS OF SHOCK—BOUNDARY-LAYER INTERACTION ON THE PERFORMANCE OF A LONG AND A SHORT SUBSONIC ANNULAR DIFFUSER

By Charles C. Wood and John R. Henry

SUMMARY

In connection with the problem of obtaining high pressure recovery and uniform exit velocity distributions for air-induction systems, an investigation was conducted to determine the effects on performance of positioning normal shocks in or upstream of both a long and a short subsonic annular diffuser. The diffuser-entrance Mach number was varied from 0.2 to that corresponding to the choked condition and was also fixed at a value of 1.44 through use of a supersonic nozzle. The shock Mach number was varied from 1.0 to 1.8. Area distributions throughout the diffuser lengths corresponded to those of 5° and 10° conical diffusers having the same entrance area and area ratio.

Total-pressure losses from shock—boundary-layer interaction for the annular diffusers were appreciably smaller than values given in the literature for conical diffusers of nearly the same expansion angles. Approximately $2\frac{1}{2}$ hydraulic diameters of constant-area ducting between the diffuser entrance and the shock resulted in equal pressure recovery for the two diffusers and the elimination of losses from shock—boundary-layer interaction. For equal shock Mach numbers, the 5° diffuser produced velocity distributions that were superior to those of the 10° diffuser; flow separation at the exit of the 5° diffuser was not observed for shock Mach numbers below approximately 1.7. Boundary-layer control would be required for both diffusers for most of the entrance flow test conditions in order to obtain exit flow distributions comparable to a 1/7-power profile.

INTRODUCTION

The performance of the turbojet and ram-jet power-plant installations in supersonic aircraft depends to a large extent on the performance

of the air-induction system of which the subsonic diffuser is an important part. Much data on subsonic-diffuser performance are available and are summarized in reference 1. Most of these data are for subsonic-entrance Mach numbers, and the entrance flow conditions to the diffusers are not typical of those established by the supersonic-entrance section; in fact, very little performance data for diffusers operating under such conditions are available. (See refs. 1 and 2.) Aircraft designers recognizing this factor as well as the importance of the subsonic diffuser have resorted to designs with extremely small expansion angles to insure satisfactory performance. In many instances, diffusers designed accordingly have penalized the aircraft design because of diffuser length and weight.

The purpose of the present report is to present for comparison purposes the experimental results of both a long and a short subsonic annular diffuser which was tested to determine the effects on performance of positioning a normal shock in or upstream of the diffuser. This investigation is part of a general program initiated to determine methods for designing shorter diffusers for use with supersonic entrances. The diffuser-entrance Mach number was varied from 0.2 to that corresponding to the choked condition and was also fixed at a value of 1.44 through use of a supersonic nozzle. The shock Mach number varied from 1.0 to 1.8. The boundary layer at the entrance occupied about 40 percent of the annulus. The maximum Reynolds number based on the hydraulic diameter of the entrance was 2.25×10^6.

SYMBOLS

A	cross-sectional area
D	outer ducting diameter
G	gap or radial distance between inner and outer walls
x	axial distance measured from cylinder-diffuser junction
M	Mach number
M_s	Mach number just upstream from normal shock
p_t	total pressure (see section entitled "Performance Parameters")
Δp_t	total-pressure loss

[redacted]

p	static pressure
Δp	static-pressure change
q	compressible dynamic pressure, $p_t - p$
R	radius of circular pipe
u	local stream velocity
U	maximum velocity in a profile at a given duct station
y	radial distance measured from inner wall
δ	boundary-layer thickness
δ^*	two-dimensional, incompressible, boundary-layer displacement thickness, $\int_0^\delta \left(1 - \frac{u}{U}\right)dy$
θ	two-dimensional, incompressible, boundary-layer momentum thickness, $\int_0^\delta \frac{u}{U}\left(1 - \frac{u}{U}\right)dy$

A bar above a symbol indicates a mean quantity.

Subscripts:

1	reference station
2	station in throat of upstream venturi meter (see fig. 1)
3	reference entrance station for diffuser (see fig. 2)
4,5,6,7	survey stations located downstream from diffuser entrance
8	station in throat of downstream venturi meter (see fig. 1)
i	inner wall of diffuser
o	outer wall of diffuser
s	shock

[redacted]

c calculated value

x axial distance, an independent variable

APPARATUS AND PROCEDURE

General Apparatus

The setup used for this investigation is illustrated in figure 1 and consisted of a 30-inch-diameter settling chamber with screens for reducing the turbulence level of the flow, an annular-entrance venturi meter, a center-body support section containing 18 struts of high fineness ratio, the diffuser model and adjacent ducting, an exit venturi meter, a section containing a butterfly control valve, and an exit diffuser. All ducting was machined to close tolerances; joints were smooth and continuous and were sealed to prevent leaks.

Two variations in the setup were tested which will be referred to herein as configurations I and II (fig. 2). The two configurations were identical with the exception of one duct section located upstream of the diffuser for configuration II. The walls of this duct section were contoured to form a supersonic nozzle, and the duct surfaces at the upstream and downstream ends of this duct section were continuous with adjacent ducting. The area ratio of the supersonic nozzle corresponded to that required for a Mach number of 1.6. The area distribution of the supersonic-nozzle section was obtained by use of two-dimensional, supersonic, characteristic procedures.

Diffuser Models

The outer wall of the two diffusers was cylindrical with a diameter of 13.5 inches. (See fig. 2.) The design of the 5° diffuser differed from that of the 10° diffuser only in the length, which was 1.87 times that of the 10° diffuser. For about 95 percent of the diffuser length, the shape of the inner bodies was such that the flow-area increase per unit length was the same as that of the 5° and 10° conical diffusers. (See fig. 3(a).) The junctions between the upstream cylinder and the upstream end of the diffuser inner bodies consisted of a circular-arc contour (see fig. 2), and the terminals of the inner bodies were arbitrary fairings. These methods of design were used at the ends of the inner bodies to avoid the sharp changes in contour that would have resulted from the area variation for an equivalent conical angle.

The longitudinal variation of the angle between a tangent to the inner-body wall and a line parallel to the diffuser axis (local expansion

angle) is given in figure 3(b) for both diffusers. The expansion angles are small near the diffuser entrance and increase rapidly with length to high values near the diffuser exit. For a given diffuser length this type of variation should minimize shock—boundary-layer interaction effects for shock locations near the diffuser entrance since increasing the wall expansion angle produces shock-induced flow separation that is more violent. (See ref. 2.) The high expansion angles near the exit would have to be compensated for by boundary-layer control in this region in order to obtain high performance.

Instrumentation

A reference total-pressure tube and a thermocouple were located in the 30-inch-diameter settling chamber. Three longitudinal rows of static-pressure orifices were equally spaced about the circumferences of the inner and outer walls in the diffusers and adjacent ducting. Three static orifices equally spaced about the circumference of the outer wall were located in the throats of the venturi meters at stations 2 and 8. Three total-pressure traversing tubes were equally spaced about the duct circumference at stations 2 to 8. (See figs. 1 and 2 for station locations.) The pressure readings of wall orifices were recorded by photographing multitube manometer boards. All data obtained from total-pressure traverses were recorded by using commercial transducer pressure cells in conjunction with electronic data plotters which limited the frequency response to 10 cycles or less and gave a continuous plot of the pressure loss from the reference tube to the survey position. In all cases traverse data were obtained to within 0.035 inch of each wall.

Test Procedure

The investigation was initiated by obtaining total-pressure traverses and static-pressure measurements at station 2 (venturi meter) for a range of duct Mach numbers from approximately 0.2 to the choked condition. The survey tubes were then removed, were reinstalled at station 3 (the reference station at the diffuser entrance), and the tests were repeated. Total-pressure traverses at stations 2 and 3 were made for the purpose of calibrating the upstream venturi meter and of determining the total-pressure distribution near the diffuser entrance. Total-pressure traversing tubes were then installed successively at the downstream stations and traverses were made for the aforementioned Mach number range and for a choked-entrance condition with a shock in the diffuser. The location of the shock was varied by regulating the back pressure. Similar measurements were made for both diffuser models in order to obtain a comparison of the flow development throughout the diffusers.

With the exception of the total-pressure traverses at station 2, the procedure described in the preceding paragraph was repeated for configuration II. For the tests of configuration II the flow at the diffuser entrance (cylinder-diffuser junction) was either supersonic at a Mach number of 1.44 or subsonic; the flow speed depended on whether the normal shock was located in the constant-area duct section preceding the diffuser entrance or in the diffuser proper.

Performance Parameters

The two diffusers tested in this investigation were compared on the basis of the following parameters: (1) total-pressure loss, (2) velocity distributions in and downstream from the diffusers, (3) total-pressure distortions at station 6, and (4) the static-pressure rise. Diffuser total-pressure loss is defined as the difference between the total pressure at station 3 and that at station 8. The total pressure at station 3 was determined by mass-weighting the survey data. Since the flow distribution at station 8 was essentially one-dimensional, the total pressure was calculated from one-dimensional relations by using the measured static pressure at station 8 and the mass flow determined from the venturi-meter measurements at station 2.

Total-pressure-loss and static-pressure-rise data for diffuser-entrance Mach numbers below choke are expressed nondimensionally by dividing them by the compressible dynamic pressure at station 3. These data are presented as a function of the mean Mach number at station 3. For cases in which the flow contained a normal shock, total-pressure loss and static-pressure rise are expressed nondimensionally by dividing them by the mean total pressure at station 3. These data are correlated against the mean Mach number of the flow just upstream from the shock wave. The shock Mach number was calculated by averaging the inner- and outer-wall static pressures immediately upstream of the shock and by using one-dimensional relations in a manner similar to that used to determine the total pressure at station 8.

Velocity distributions are presented as the ratio of the local velocity to the maximum velocity occurring in the same cross-sectional plane. Total-pressure distortion is defined as the ratio of the difference between the maximum and minimum total pressure to the mean total pressure at station 8. The minimum total pressure was defined as that measured at a point 5 percent of the width of the duct gap from the inner wall. Values of M_6 corresponding to the data points of total-pressure distortion were calculated for a uniform flow by using one-dimensional relations and the total pressure measured at station 8.

RESULTS AND DISCUSSION

Entrance Flow Conditions

Velocity and Mach number distributions determined from traverses at station 3 are presented in figure 4 for both configurations I and II. Values presented are averaged data from the three total-pressure tubes spaced about the circumference. Data presented for configuration I are for two speeds: a choked-entrance condition and a lower Mach number. For configuration I the entrance Mach number had little effect on the velocity distribution at station 3. The boundary layer at each wall extended over about 20 percent of the gap. The velocities adjacent to the inner and outer walls were about 80 and 60 percent of the maximum velocity, respectively.

Data are presented in figure 4(b) for test configuration II with the normal shock located both upstream and downstream of station 3. With the shock downstream from station 3, the boundary-layer thickness on the outer wall extended over 21 percent of the gap as compared with 18 percent for the inner wall. The relative velocities adjacent to the walls were similar in magnitude to those for configuration I. The maximum Mach number at station 3 was approximately 1.5. With the shock upstream of station 3, the flow was distorted and the boundary layer extended across the entire flow. The boundary layer in the immediate vicinity of the shock was probably separated; however, reattachment occurred before the flow reached station 3.

Velocity distributions for the three individual survey locations at station 3 for configurations I and II are presented in figure 5. Also presented are values of boundary-layer displacement thickness and of shape parameter δ^*/θ obtained by averaging data for the three surveys. Differences in the velocity distributions for the three locations are insignificant for all the flow conditions. Values of shape parameter for both the inner and outer walls for all test conditions are low, which indicates that the boundary-layer velocity distributions were favorable toward subsequent flow diffusion.

Performance for Subsonic-Entrance Flows

Velocity distribution.- Velocity distributions measured at station 7, a short distance downstream from the diffuser exit, for both diffuser models are presented in figure 6(a) for several Mach numbers from approximately 0.31 to the choking Mach number. Distributions for both models were badly distorted; the boundary layer was thickest at the inner wall and extended over approximately 65 percent of the duct radius. The 5° diffuser produced the most uniform flow. Increasing the entrance Mach number

had no apparent effect on the velocity distribution for the 5° diffuser but was unfavorable for the 10° diffuser.

Figure 6(b) presents additional velocity distributions determined from measurements at several stations in the 10° diffuser. The boundary layer extended across the entire duct from station 5 to the exit, and the velocities near the walls ranged from 20 percent to 45 percent of the maximum for stations 5 to 7. At stations 6 and 7 the distributions were not symmetrical.

Total-pressure-loss and static-pressure-rise coefficients.- The loss in total pressure between stations 3 and 8 and the static-pressure rise between stations 3 and 7 are presented nondimensionally in figure 7 as functions of the entrance Mach number. Also included in the figure is the theoretical, isentropic, one-dimensional, static-pressure-rise coefficient. The loss coefficients for the two models are approximately equal at the higher Mach numbers, but the 10° diffuser produced slightly less loss at lower Mach numbers. The loss coefficient for the 5° diffuser was independent of Mach number for the speed range tested. The static-pressure-rise coefficient for both diffusers increased with increasing Mach number; the static-pressure rise for the 5° diffuser was larger than that for the 10° diffuser, probably because the 5° diffuser had a more uniform exit-velocity profile as shown in figure 6(a). The 5° diffuser recovered about 85 percent of the theoretical static-pressure rise. The performance values for both models are typical for these geometries.

Longitudinal static-pressure distribution.- The nondimensional static-pressure rise along both the inner and outer walls for the two diffuser models is presented in figure 8 for two speed conditions. The data show that the static-pressure rise downstream from the center body for the 10° diffuser was two to four times that for the 5° diffuser. This result probably is due to the fact that the exit velocity distribution for the 10° diffuser was more distorted than that for the 5° diffuser and, therefore, could recover more static pressure through natural mixing in the tailpipe. The static-pressure rise to the point corresponding to $x/D = 3.52$ (5° diffuser exit) is approximately the same for both models, a condition indicating that the total-pressure losses and velocity distributions are about the same at this point for both models.

Performance With Choked- and Supersonic-Entrance Flows

Velocity distributions with choked-entrance flow.- Velocity distributions at stations 4, 6, and 7 for the choked-entrance flow condition (configuration I) and shock waves at several locations in the diffuser are presented in figure 9. Flow separation was not observed at any of the three survey stations for the 5° diffuser. Station 4 was less than 1 inch downstream from the shock position for a Mach number of 1.56, and

in this case the relative velocities in the vicinity of the walls were very low. However, between stations 4 and 6 these low relative velocities increased to the point where the distribution for $M_s = 1.56$ was approximately the same as that for all other Mach numbers. The flows at stations 4 and 6 were approximately symmetrical; however, the boundary layer occupied the entire duct at station 6 as compared with about 70 percent of the duct at station 4. A comparison of the distributions in figure 9 with the 1/7-power profile shows that all the distributions were less uniform than that for fully developed pipe flow. The distributions at station 7 show that the peak-velocity point occurred at approximately 65 percent of the duct radius and that the velocities immediately adjacent to both the inner and outer walls were approximately 50 percent of the maximum velocity. The shock Mach number for the range tested (M_s from 1.02 to 1.53) had little effect on flow uniformity.

The distributions produced by the 10° diffuser were noticeably less uniform than those for the 5° diffuser, and flow separation from the inner wall occurred upstream of station 4 for a shock Mach number of 1.45. Flow separation was not observed at station 7 because of natural mixing of flow between the diffuser exit and station 7.

Velocity distributions with supersonic-entrance flow.- Velocity distributions at station 6 for configuration II are presented in figure 10(a) for shock Mach numbers up to 1.79. For configuration II, shocks were positioned in several locations in the constant-area duct upstream from the diffuser entrance as well as in the diffuser proper. The mean Mach number in the constant-area section varied from 1.6 at the nozzle exit to 1.44 at the diffuser entrance. The three curves for each diffuser model with the highest velocities near the inner wall correspond to shock locations in the constant-area duct section.

The velocity distributions for the 5° diffuser became progressively less uniform as the shock moved from an upstream location in the constant-area duct through the constant-area duct and into the diffuser. Flow separation from the inner wall was present at station 6 at a shock Mach number of 1.75. The flow was approximately symmetrical when the shock occurred in the constant-area section; however, the boundary layer extended almost to the center of the annular passage. For these cases the distributions were approximately equivalent to that for a 1/7-power profile.

Distributions for the 10° diffuser were considerably less uniform than those for the 5° diffuser. Flow separation from the inner wall occurred for all test conditions for which the shock was located in the diffuser and immediately upstream of the diffuser entrance. Location of the shock in the constant-area section approximately $1\frac{1}{2}$ entrance

[redacted]

hydraulic diameters (hydraulic diameter is defined as a quantity that is four times the cross-sectional area divided by the wetted perimeter) upstream from the diffuser entrance resulted in no separation at station 6; however, the distribution was far from uniform. On the basis of data presented herein it appears that, except for the case where shocks were located upstream from the 5° diffuser, boundary-layer control would be required for both diffusers for all entrance flow conditions tested in order to obtain exit flow distributions comparable to a 1/7-power profile.

Total-pressure distortion.- Data taken at station 6 are presented as a function of shock Mach number in figure 10(b). The value of $p_{t,min}$ contained in the distortion coefficient was taken at a distance from the inner wall equal to 5 percent of the gap width since, for the majority of tests conducted, the flow energy adjacent to the inner wall was lowest. The trends indicated by the various curves are the same as those noted in the discussion of velocity distributions. The maximum total-pressure distortion for configuration I and the 10° diffuser ranged from $0.15\bar{p}_{t,8}$ at a shock Mach number of 1.0 to a value of $0.52\bar{p}_{t,8}$ at a shock Mach number of 1.58. The total-pressure distortion for configuration I and the 5° diffuser was approximately $0.085\bar{p}_{t,8}$ and varied little with Mach number. At a given shock Mach number the total-pressure distortions observed for configuration II are less than distortions observed for test configuration I. This result was probably obtained because for configuration II the diffuser area ratio from the shock to station 6 was larger and, consequently, the Mach number at station 6 was smaller. A maximum distortion factor of 0.82 (configuration II; 10° diffuser) was measured. This value appears to be very high because the maximum and minimum total pressures correspond to Mach numbers of approximately 1.0 and 0, respectively, and because the maximum total pressure was appreciably higher than that at station 8. A 1/7-power profile would correspond approximately to a 4-percent distortion for a Mach number in the range from 0.30 to 0.35; this profile, as noted in the discussion of the velocity distributions, was obtained only for configuration II with the 5° diffuser with the shocks upstream from the diffuser entrance.

Total-pressure loss.- The total-pressure-loss coefficient for the two diffusers for configurations I and II is plotted as a function of shock Mach number in figure 11(a). The total-pressure loss is defined as the difference between the total pressure just upstream from the shock location and the total pressure at station 8. The total pressure just upstream from the shock location was determined from the measured total pressure at station 3 (for the cases where no shock was located upstream) and from calculations of the friction loss between station 3 and the various shock locations. The friction-loss calculations were performed by using equations (6) and (7) of reference 3 and friction factors for a smooth pipe taken from reference 4. For the cases where the shock was

[redacted]

located in the diffuser proper, the friction calculation was performed by assuming that the cross-sectional-area increase occurred in a series of incremental steps. This procedure was adopted in order to utilize the equations of reference 3, which are for a constant-area duct. The maximum friction loss calculated was about 7 percent of the total pressure and corresponded to the highest shock Mach number for the 5° diffuser and configuration II.

Figure 11(a) also presents the one-dimensional, normal-shock, total-pressure loss. The normal-diffuser-loss increments, which have been added to the normal-shock curve, represent the loss that would be expected to occur in the subsonic-diffuser flow with no normal shock present. The normal diffuser losses were obtained by modifying the subsonic test data of configuration I to correspond with the diffuser area ratio available downstream from the shock location and to correspond with the theoretical Mach number downstream from the shock. The modification was accomplished by using correlation procedures described in reference 1.

At a Mach number of 1.0 the 5° and 10° diffusers produced equal total-pressure losses because the higher diffusion losses of the 10° diffuser were apparently exactly balanced by the higher friction losses of the 5° diffuser. However, as the shock Mach number increased, the loss of the 10° diffuser increased at a much higher rate than that of the 5° diffuser and reached a value of $0.274\bar{p}_{t,3}$ at a shock Mach number of 1.69. The measured losses for both diffusers were significantly higher than the sum of the one-dimensional, normal-shock loss and the normal diffuser loss. This difference in loss is considered herein to be excessive diffuser loss resulting from shock-wave—boundary-layer interaction. For the same shock Mach number the losses obtained for the two diffusers with configuration II (supersonic-entrance flow condition) are either the same or slightly higher than those obtained with configuration I with the exception of cases in which the normal shock occurred in the constant-area section upstream from the diffuser.

The effect of a length of constant-area ducting between the shock and the cylinder-diffuser junction is best illustrated in figure 11(b) where total-pressure losses are presented as a function of the duct length in terms of entrance hydraulic diameters. The one-dimensional, normal-shock loss varies with shock location in the constant-area section because of a Mach number variation resulting from friction. Increases in the constant-area duct length between the shock and diffuser entrance resulted in rapid decreases in total-pressure loss for the 10° diffuser; the loss changed from $0.163\bar{p}_{t,3}$ with the shock located 0.17 hydraulic diameter upstream to a value of $0.120\bar{p}_{t,3}$ at a shock location of -2.65 hydraulic diameters. For the 5° diffuser the effect of distance between the shock and the cylinder-diffuser junction on the loss was much less than that for the 10° diffuser, and a minimum loss was obtained

[redacted]

with about 1 hydraulic diameter of duct length. With approximately 2.5 hydraulic diameters of duct length, the losses of the two diffusers were nearly equal and were greater than the sum of the normal diffuser loss and the one-dimensional, normal-shock loss by about 1 percent to 2 percent of $\bar{p}_{t,3}$. A study of the data of reference 2 shows that these differences of 1 percent to 2 percent are equal to the effect of boundary layer on the normal-shock losses in a constant-area duct.

Comprehensive data concerning the use of a constant-area duct section for improving conical-diffuser performance are available in reference 2, in which shock waves were always located in the constant-area duct passage preceding the diffuser entrance. Data were obtained for a range of shock Mach numbers from 1.76 to 2.51 and for a range of boundary-layer thickness. The data of reference 2 substantiate trends indicated by data for the annular diffusers; the total-pressure losses were a minimum with the shock wave located in the constant-area passage a sufficient distance upstream from the diffuser entrance to permit the normal-shock-wave static-pressure rise to occur upstream of the diffuser entrance. Approximate values of loss coefficient obtained by extrapolating the data of reference 2 to a Mach number of 1.44 are given in figure 11 for both the 6° and 12° conical diffusers for the case in which the upstream end of the normal shock was located at the diffuser entrance. The point for the 6° conical diffuser falls on the curve for the 10° annular diffuser, and the point for the 12° conical diffuser lies considerably above all the other data. The fact that the conical-diffuser losses are higher than the annular-diffuser losses for nearly the same nominal expansion angle probably can be attributed to the annular-diffuser wall angles being appreciably less than the nominal expansion angle in the upstream part of the diffusers where the shock pressure rise took place. (See fig. 3(b).)

Losses from shock—boundary-layer interaction.- The total-pressure losses resulting from shock—boundary-layer interaction as determined from the curves of figure 11(a) are presented in figure 12 as a function of shock Mach number. Also included are curves of similar losses from data on several induction-system designs which are summarized in reference 1. The two curves which have been extracted from reference 1 correspond to conical spike-type entrances having no internal contraction. The models were of small scale and were operating critically with the normal shock positioned just downstream from the minimum-area station. The current 5° diffuser data agree with the data of reference 1 for 3° to 5° within about 2 percent of the total pressure; however, the data of reference 1 are invariant with Mach number, whereas the current data indicate a progressively increasing loss with Mach number. The losses of total pressure from shock—boundary-layer interaction for the 10° annular diffuser are from 2 percent to 4 percent lower than those of the 9.4° curve of reference 1. In general, the current data are more reliable than those of reference 1; in reference 1 the losses up to the

terminal shock had to be estimated, and differences in the geometries and test procedures of the several investigations of reference 1 resulted in considerable data scatter. The two data points which were obtained from reference 2 are also presented in figure 12. The conical-diffuser shock-induced losses are higher than those of the annular diffuser as discussed previously.

Longitudinal static-pressure distribution.- The longitudinal wall static-pressure distributions for both configurations and diffuser models are presented in figures 13 to 16 for conditions in which a normal shock was located in or upstream from the diffuser. Each figure contains a single curve for which the values of $p_x/\bar{p}_{t,3}$ tend to become smaller as x/D increases. This curve represents the locus of the values of $p_x/\bar{p}_{t,3}$ obtained in the flow upstream from the normal-shock locations. Each of the curves which branch off from the locus curve represents the increases in static pressure obtained downstream from the particular normal shocks noted in the legends. The static-pressure rises obtained on the latter curves were produced by a combination of the normal-shock static-pressure rise and the subsonic diffusion. In every case the shock pressure rise extended over an appreciable distance along the walls because of the inability of the boundary layer to absorb abrupt increases in pressure. (See ref. 2.) At the higher shock Mach numbers the pressure distributions were frequently irregular because of flow separations and irregular shock patterns.

Theoretical pressure rise through shocks and diffusers.- The data of figures 13 to 16 were analysed further to determine the amount of theoretical pressure rise actually recovered in the diffusers. In connection with this analysis the theoretical, one-dimensional, pressure rises due to the normal shocks and the isentropic, one-dimensional, pressure rises due to the subsonic diffusion were computed and are presented in figure 17 as a function of shock Mach number. The lowest curve of figure 17 is drawn through test data for configuration I for both the 5° and 10° diffusers and for configuration II for the 5° diffuser; this curve represents the values of the ratio of the static pressure on the outer wall at the shock location to the mean entrance total pressure. The data of the 10° diffuser for configuration II were omitted because of the irregular character of the data as shown in figure 16. The middle curve in figure 17 represents the pressure that should be obtained after the normal-shock pressure rise according to one-dimensional flow. The top curves represent the theoretical pressure at the end of the diffusers and include the normal-shock pressure rise and the isentropic subsonic-diffuser pressure rise from the shock location to the diffuser exit. The final theoretical pressure ratio for configuration II is slightly higher than that of configuration I because the area ratio of the subsonic diffuser downstream from the shock locations was greater for configuration II. The top curves show that the theoretical pressure

decreases appreciably with increasing shock Mach number because of the increasing total-pressure loss through the normal shock.

Diffuser lengths required to recover theoretical static-pressure rise.- The values from the top curves in figure 17 were used in conjunction with measured pressure ratios on the outer wall from figures 13 to 15 to construct the curves of figure 18. In figure 18 the increment of diffuser length, defined as the distance from the shock location to some downstream point that is required to obtain certain fractions of the theoretical static-pressure rise $\frac{\Delta p_o}{\Delta p_c}$, is presented as a function of shock Mach number. For configuration I at a shock Mach number of 1.6 the 5° diffuser recovered 80 percent of the theoretical pressure rise at the center-body terminal; whereas the 10° diffuser recovered only about 56 percent. The 5° diffuser recovered the theoretical normal-shock pressure rise well within the diffuser length for all Mach numbers; whereas the 10° diffuser was limited to a Mach number of 1.5 in this respect. For configuration II the 5° diffuser recovered the normal-shock pressure rise within the diffuser length up to a Mach number of 1.72. A comparison of the data for configurations I and II shows that a given pressure recovery occurred in a slightly shorter diffuser length for configuration II.

The length of diffuser required to recover the one-dimensional, theoretical, normal-shock pressure rise is compared in figure 19 with the length of constant-area circular pipe required to recover the maximum pressure rise downstream from a normal shock. The circular-pipe data were taken from reference 2 for the same boundary-layer displacement thickness as that measured at the entrance to the diffusers. In making the comparison the diffuser lengths were nondimensionalized by dividing them by the average gap of the annulus in the region over which the shock pressure rise occurred. This method was used because the flow near the upstream part of the diffusers was considered to be roughly two-dimensional with a width equal to the annulus gap. As the point where the shock pressure rise is completed approaches the downstream ends of the diffusers, the correlation of annulus gap with pipe diameter breaks down since the diffuser exit is a circle. The point where the data of reference 2 and the diffuser data are most comparable occurs at a shock Mach number of 1.49 for configuration II for the 5° diffuser. For this case more than half of the shock pressure rise occurred in the constant-area annulus upstream from the diffuser, and a nondimensional length of 6.0 was obtained compared with 6.6 for the circular pipe. The close agreement of the values probably indicates that annulus gap is a satisfactory correlating parameter for annular flows that are approximately two-dimensional. The diffuser static-pressure rise which is treated herein as being equivalent to the theoretical normal-shock pressure rise was effected in actuality by both the normal shock and part of the

subsonic diffusion; thus, it is not strictly comparable to the circular-pipe data. This may account for the required diffuser lengths being shorter than those for the circular pipe.

CONCLUSIONS

An investigation was conducted to determine the effects on the performance of positioning normal shocks in or upstream of both a long and a short subsonic annular diffuser. The diffuser-entrance Mach number was varied from 0.2 to that corresponding to the choked condition and was also fixed at a value of 1.44 through use of a supersonic nozzle. The shock Mach numbers varied from 1.0 to 1.8. Area distributions throughout the diffuser lengths corresponded to those of 5° and 10° conical diffusers having the same entrance area and area ratio. The following conclusions were derived:

1. The total-pressure-loss coefficients for the subsonic-entrance flow conditions were approximately the same for the two diffusers at high subsonic Mach numbers; however, the 5° diffuser produced a somewhat greater static-pressure rise and a more uniform exit velocity distribution. Variations of entrance Mach numbers below choke did not appreciably affect diffuser performance.

2. Total-pressure losses from shock—boundary-layer interaction were appreciably smaller than values given in the literature for conical diffusers of nearly the same expansion angles.

3. For the supersonic-entrance flow condition the location of a length of constant-area duct section between the diffuser entrance and the normal shock was beneficial from the standpoint of reducing total-pressure losses and improving the uniformity of exit velocity distributions. Approximately $2\frac{1}{2}$ hydraulic diameters of constant-area ducting between the diffuser entrance and the shock resulted in equal pressure recoveries for the two diffusers and the elimination of losses from shock—boundary-layer interaction.

4. A static-pressure rise equivalent to that for the theoretical normal shock was recovered within the diffuser length for shock Mach numbers up to 1.72 for the 5° diffuser (supersonic-entrance flow condition) and for shock Mach numbers up to 1.5 for the 10° diffuser (choked-entrance condition).

5. For the choked- and supersonic-entrance flow conditions for equal shock Mach numbers the 5° diffuser produced velocity distributions that were superior to those of the 10° diffuser. Flow separation at the exit

[redacted]

of the 5° diffuser was not observed for shock Mach numbers below approximately 1.75. For the supersonic-entrance flow test condition, flow separation for the 10° diffuser occurred for all shock Mach numbers except those corresponding to shock locations in the constant-area passage approximately $1\frac{1}{2}$ hydraulic diameters from the entrance. For the case of a choked-entrance condition, flow separation at the exit of the 10° diffuser was not observed for shock Mach numbers of less than approximately 1.45.

6. In order to obtain exit flow distributions comparable to a 1/7-power profile, boundary-layer control would be required for both diffusers for all the entrance flow test conditions except for the 5° diffuser operating at an entrance Mach number of 1.44 with the normal shock upstream from the diffuser.

Langley Aeronautical Laboratory,
National Advisory Committee for Aeronautics,
Langley Field, Va., January 14, 1958.

REFERENCES

1. Henry, John R., Wood, Charles C., and Wilbur, Stafford W.: Summary of Subsonic-Diffuser Data. NACA RM L56F05, 1956.

2. McLafferty, G. H., Krasnoff, E. L., Ranard, E. D., Rose, W. G., and Vergara, R. D.: Investigation of Turbojet Inlet Design Parameters. Rep. R-0790-13, United Aircraft Corp. Res. Dept., Dec. 1955.

3. Henry, John R.: One-Dimensional, Compressible, Viscous Flow Relations Applicable to Flow in a Ducted Helicopter Blade. NACA TN 3089, 1953.

4. Henry, John R.: Design of Power-Plant Installations. Pressure-Loss Characteristics of Duct Components. NACA WR L-208, 1944. (Formerly NACA ARR L4F26.)

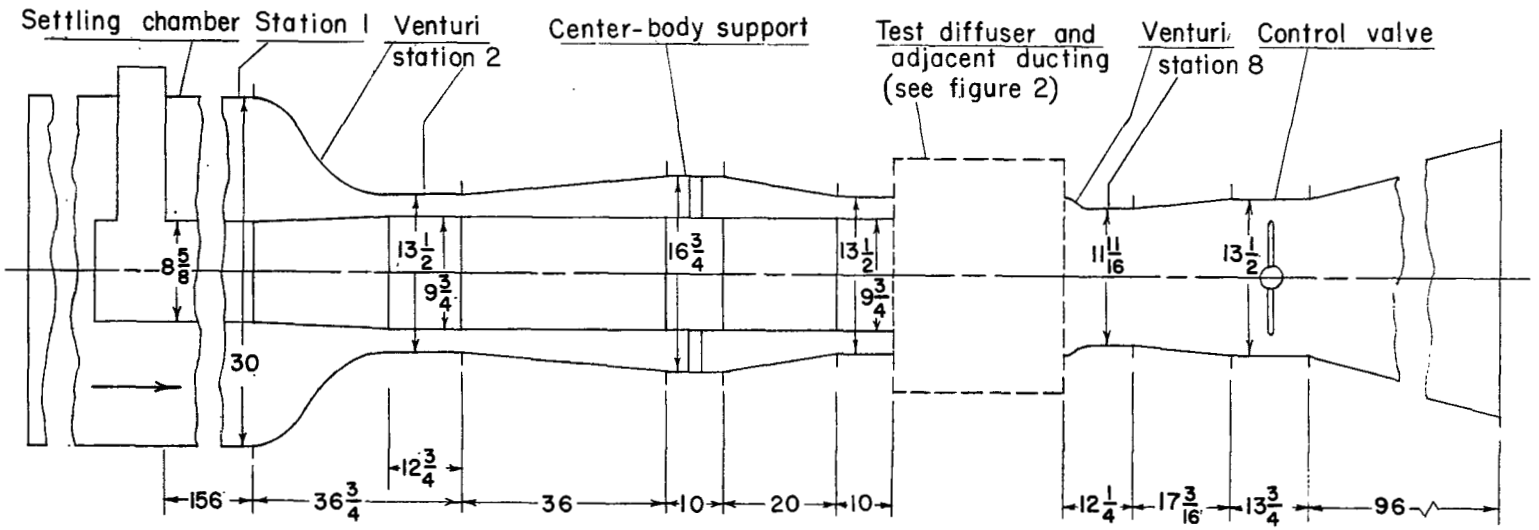

Figure 1.- Diagram of test setup. All dimensions are in inches.

Coordinates for 5° diffuser

x	y	x	y	x	y	x	y
0.0	4.875	6.250	4.610	30.250	3.133	46.750	0.829
0.062	4.875	10.250	4.415	37.250	2.464	47.950	0.0
2.250	4.790	15.250	4.150	41.250	1.961		
4.250	4.701	22.250	3.725	45.250	1.249		

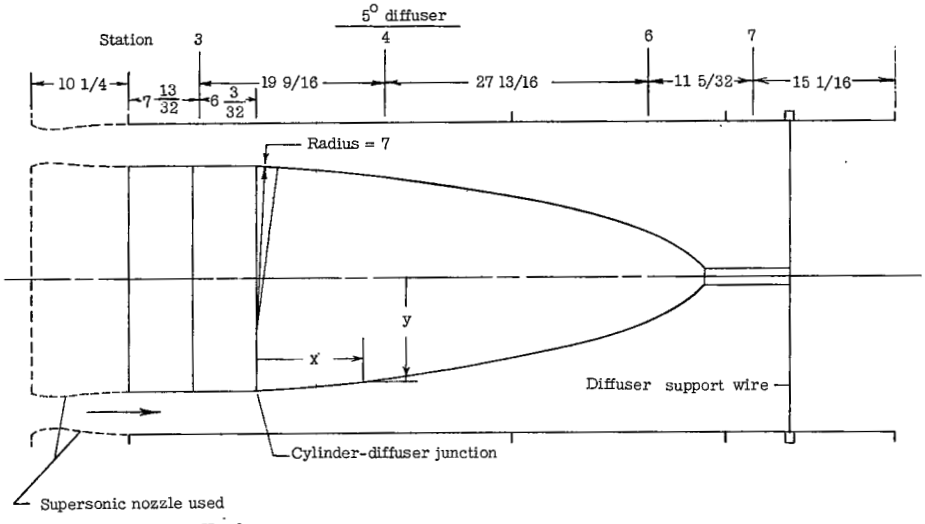

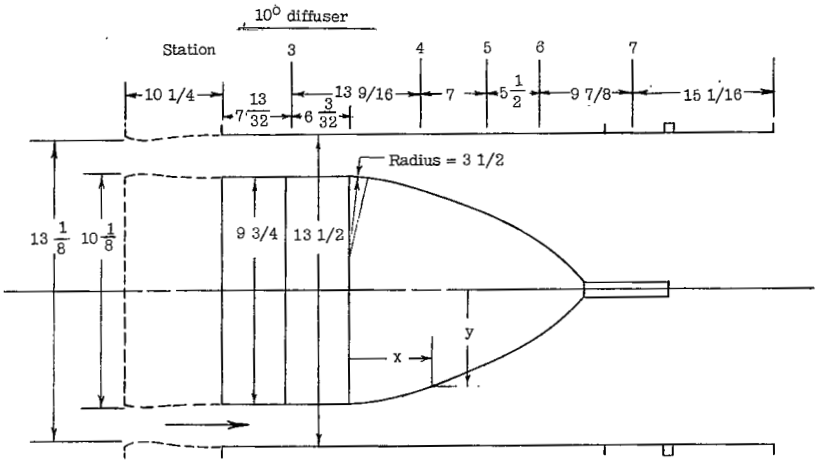

Coordinates for 10° diffuser

x	y	x	y	x	y
0.0	4.875	6.250	4.312	22.250	1.445
0.062	4.875	10.250	3.851	23.250	1.040
2.250	4.701	14.250	3.291	25.350	0.0
4.250	4.514	18.250	2.565		

Figure 2.- Diagrams of diffuser models and ducting contained within dashed-line square in figure 1. All dimensions are in inches. Configuration I is indicated by the solid lines, and configuration II is indicated by the combination of solid and dashed lines.

[redacted]

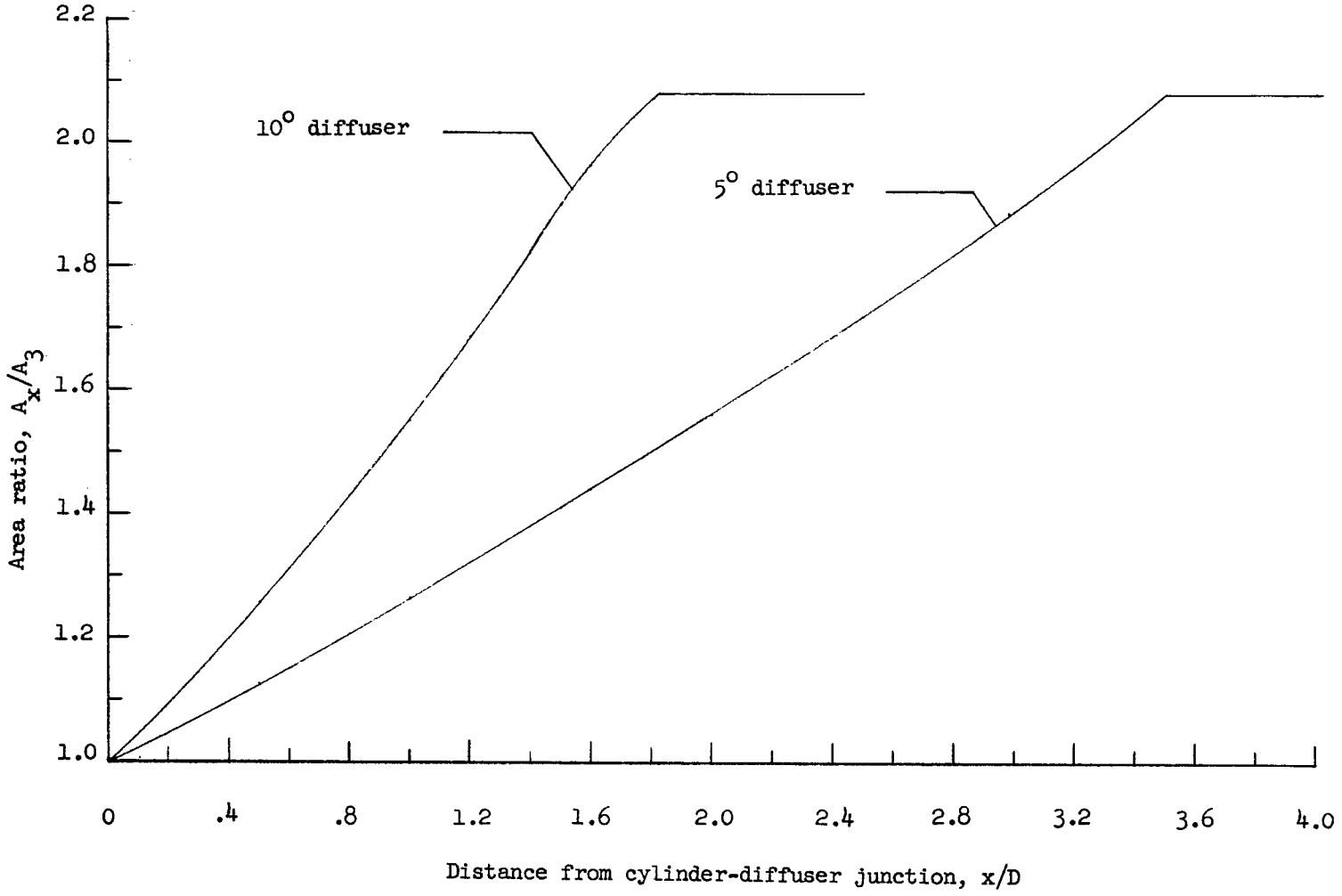

(a) Area distributions.

Figure 3.- Area distributions and expansion angles for diffuser models.

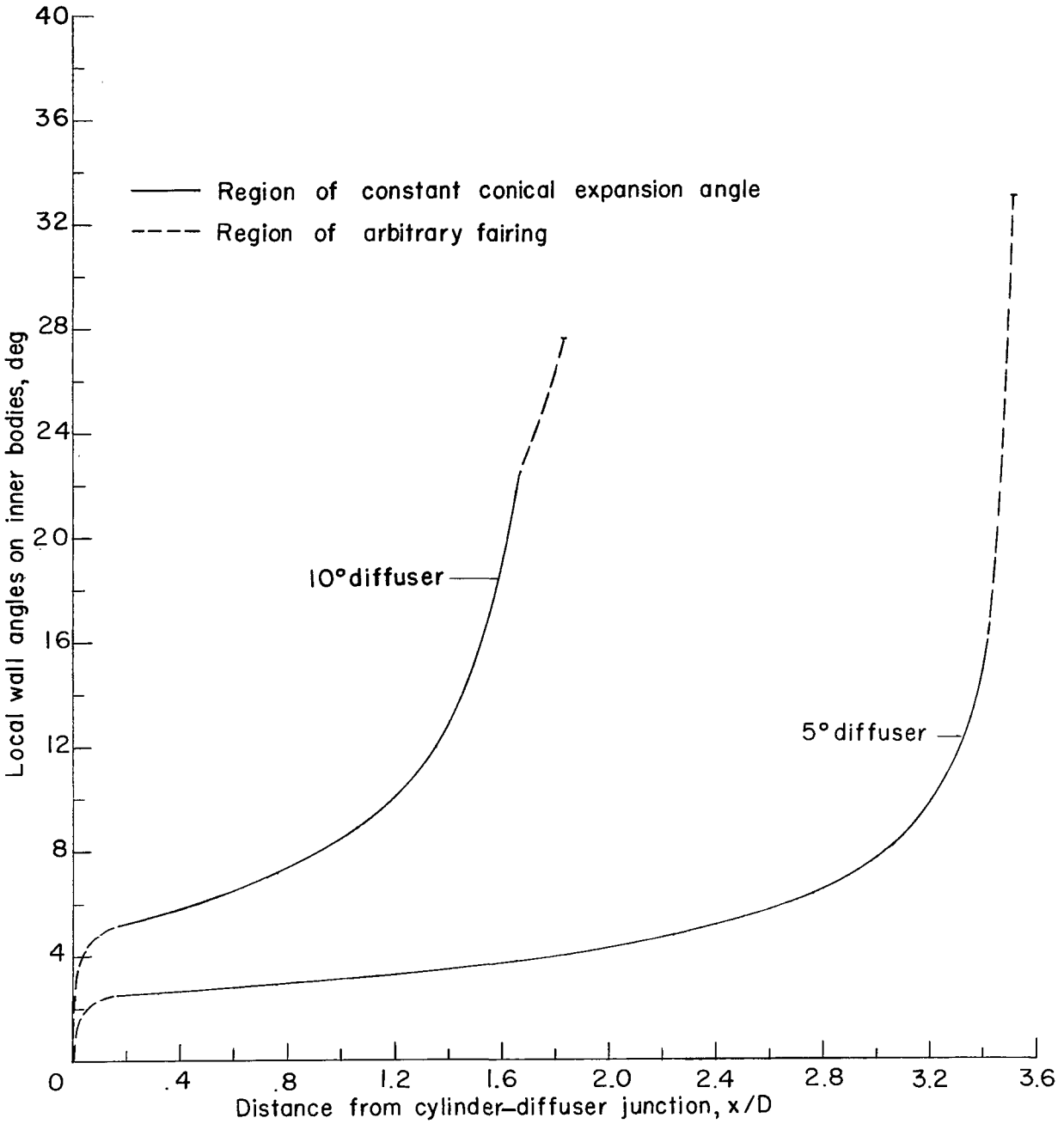

(b) Variation of local diffuser wall angle throughout the diffuser length.

Figure 3.- Concluded.

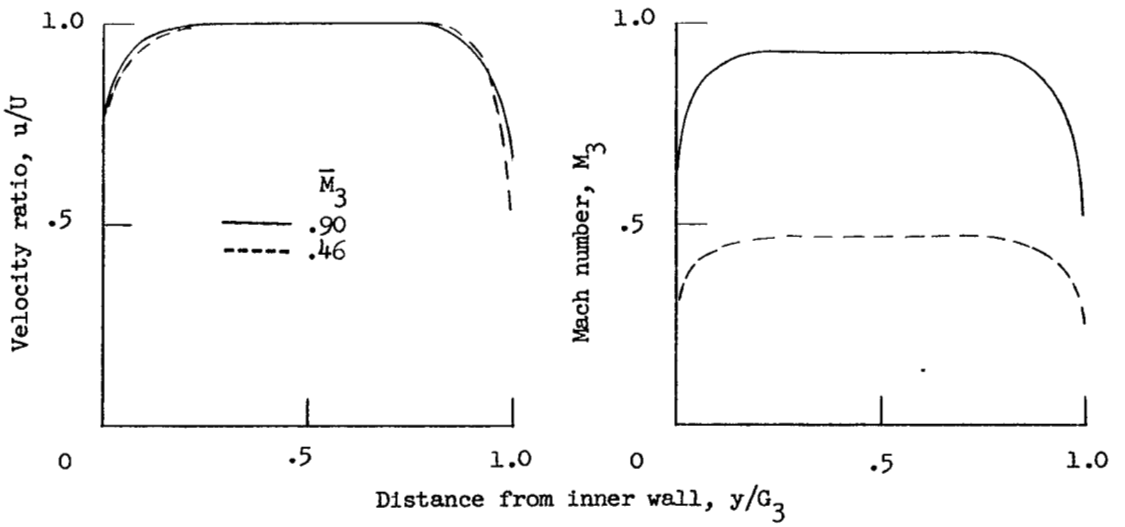

(a) Distributions for configuration I.

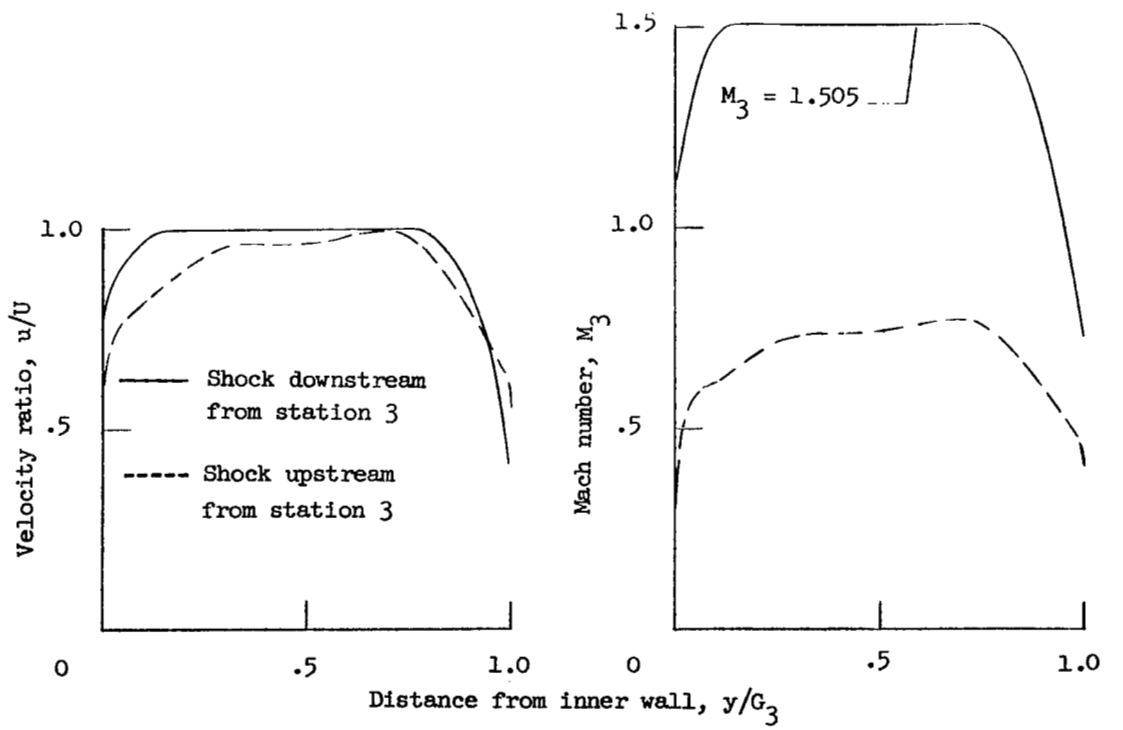

(b) Distributions for configuration II.

Figure 4.- Velocity and Mach number distributions at station 3.

[redacted]

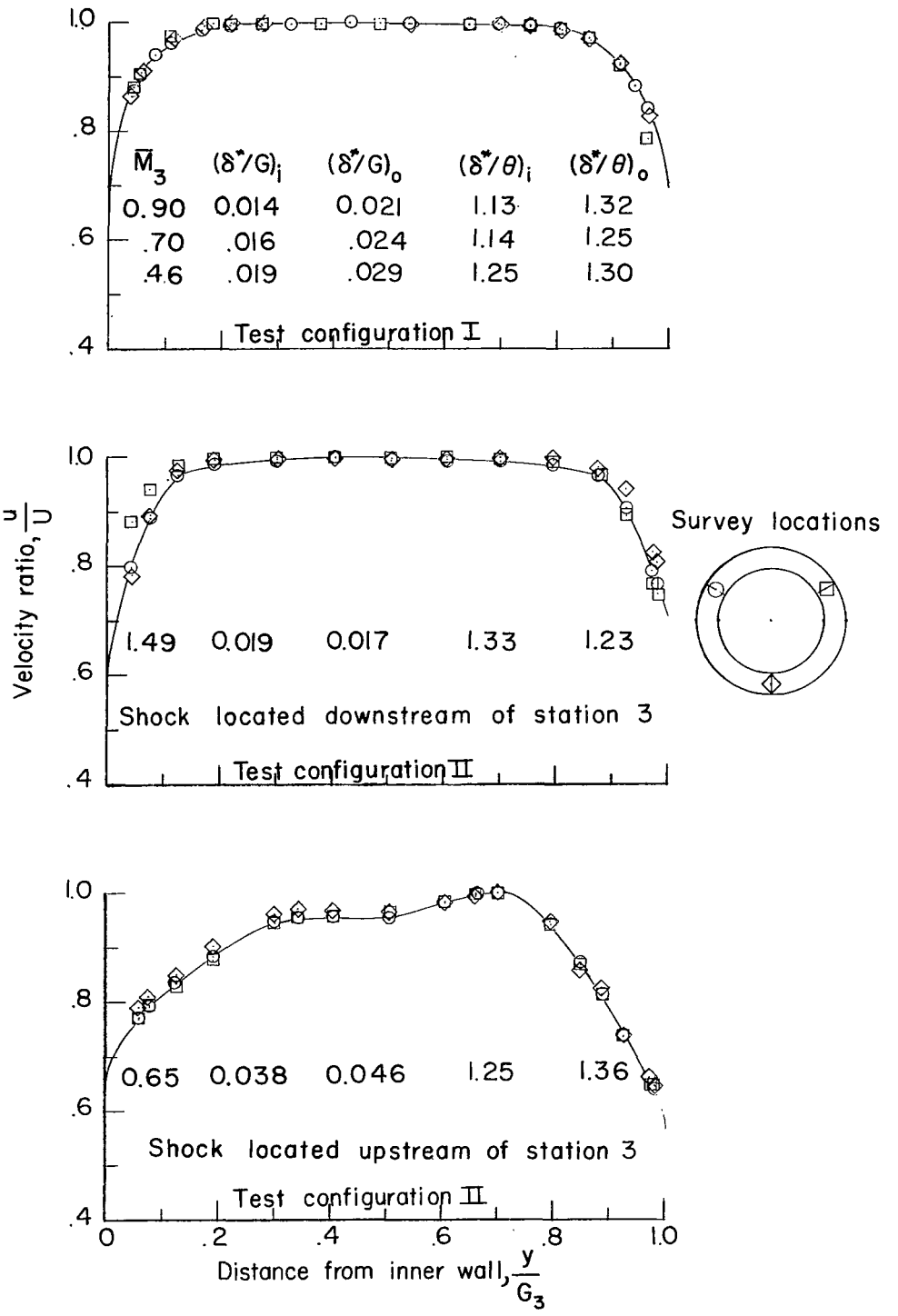

Figure 5.- Velocity distributions at station 3.

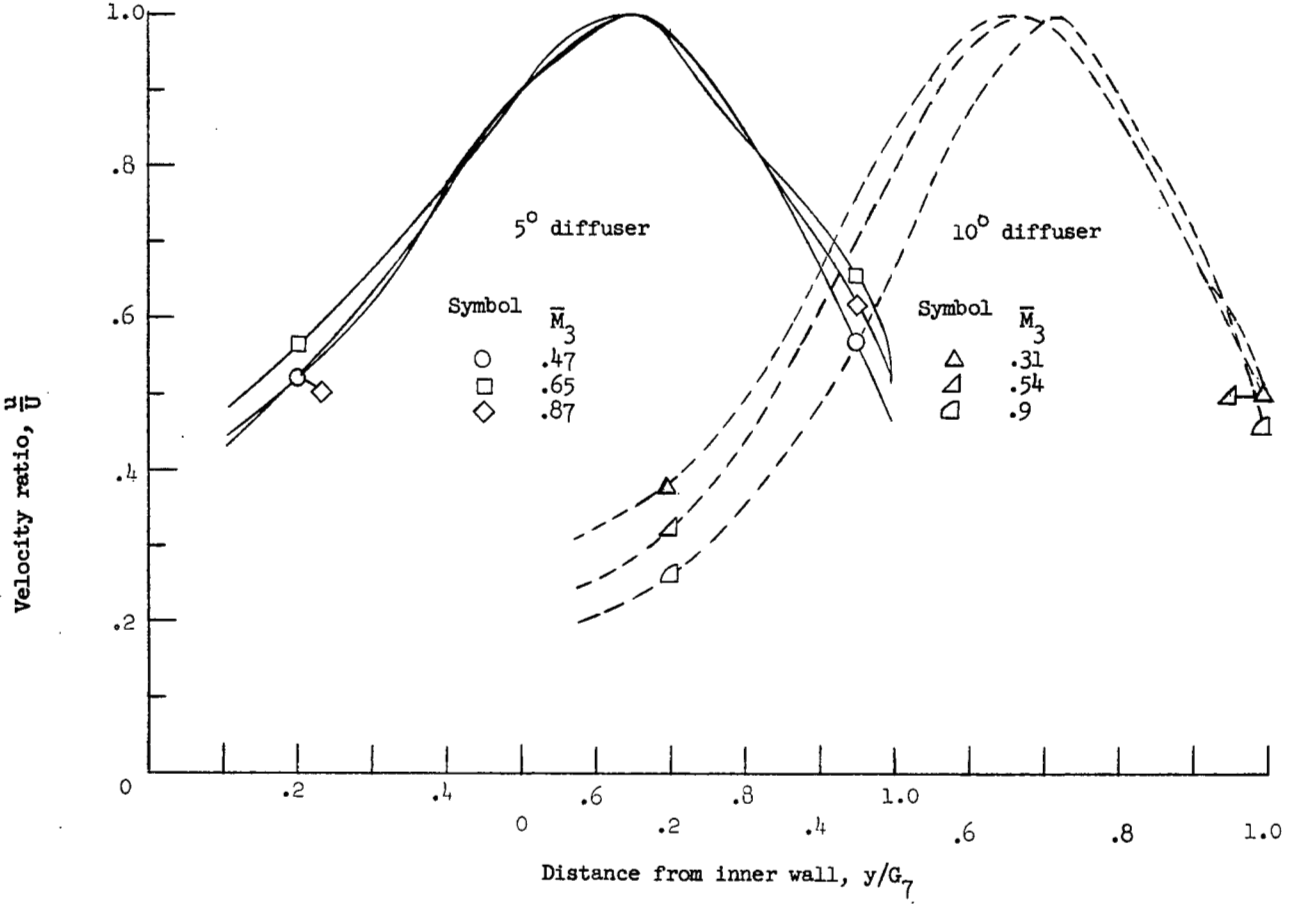

(a) Station 7.

Figure 6.- Velocity distributions for configuration I. Subsonic-flow condition.

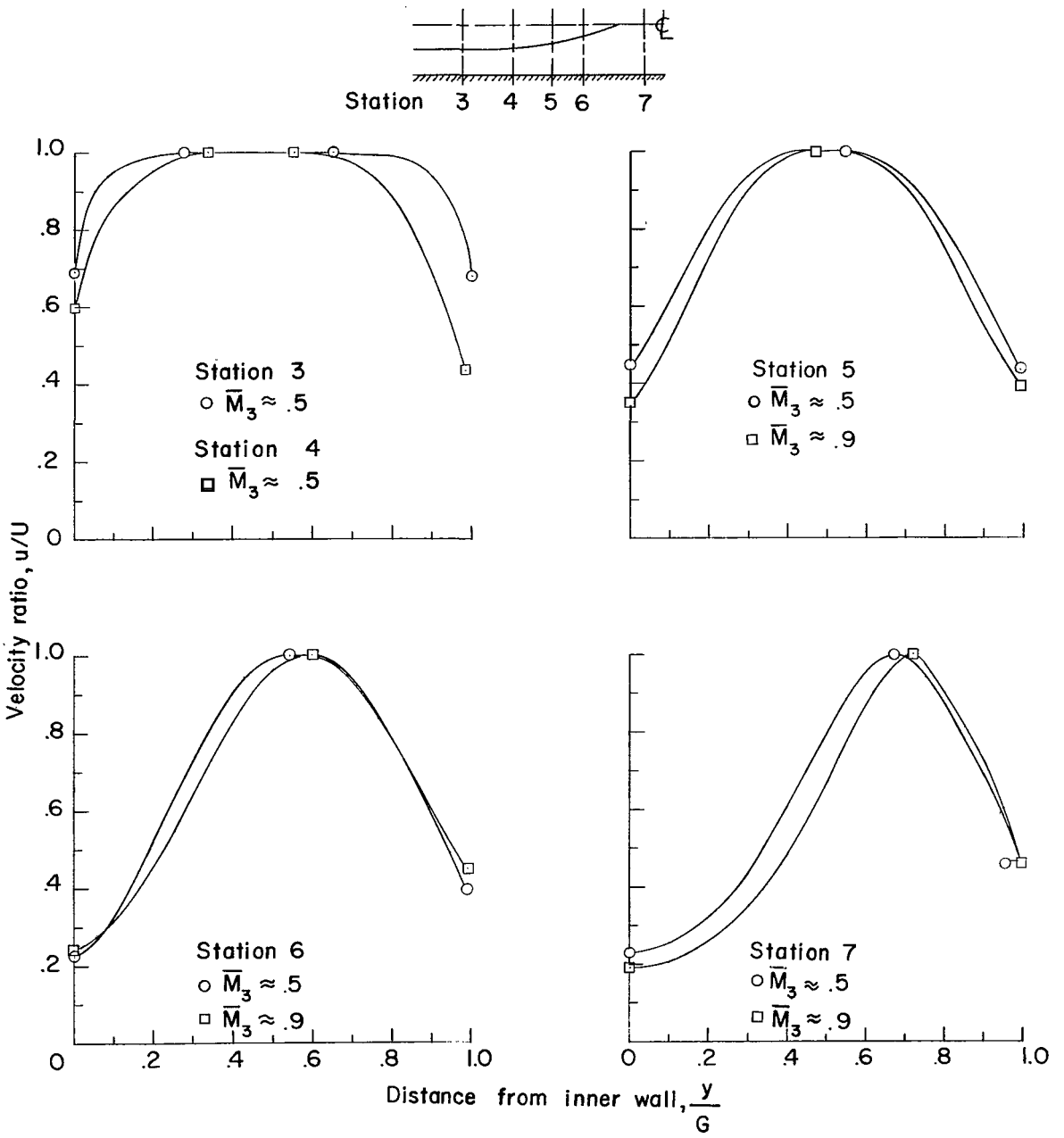

(b) Stations 3 to 7; 10° diffuser.

Figure 6.- Concluded.

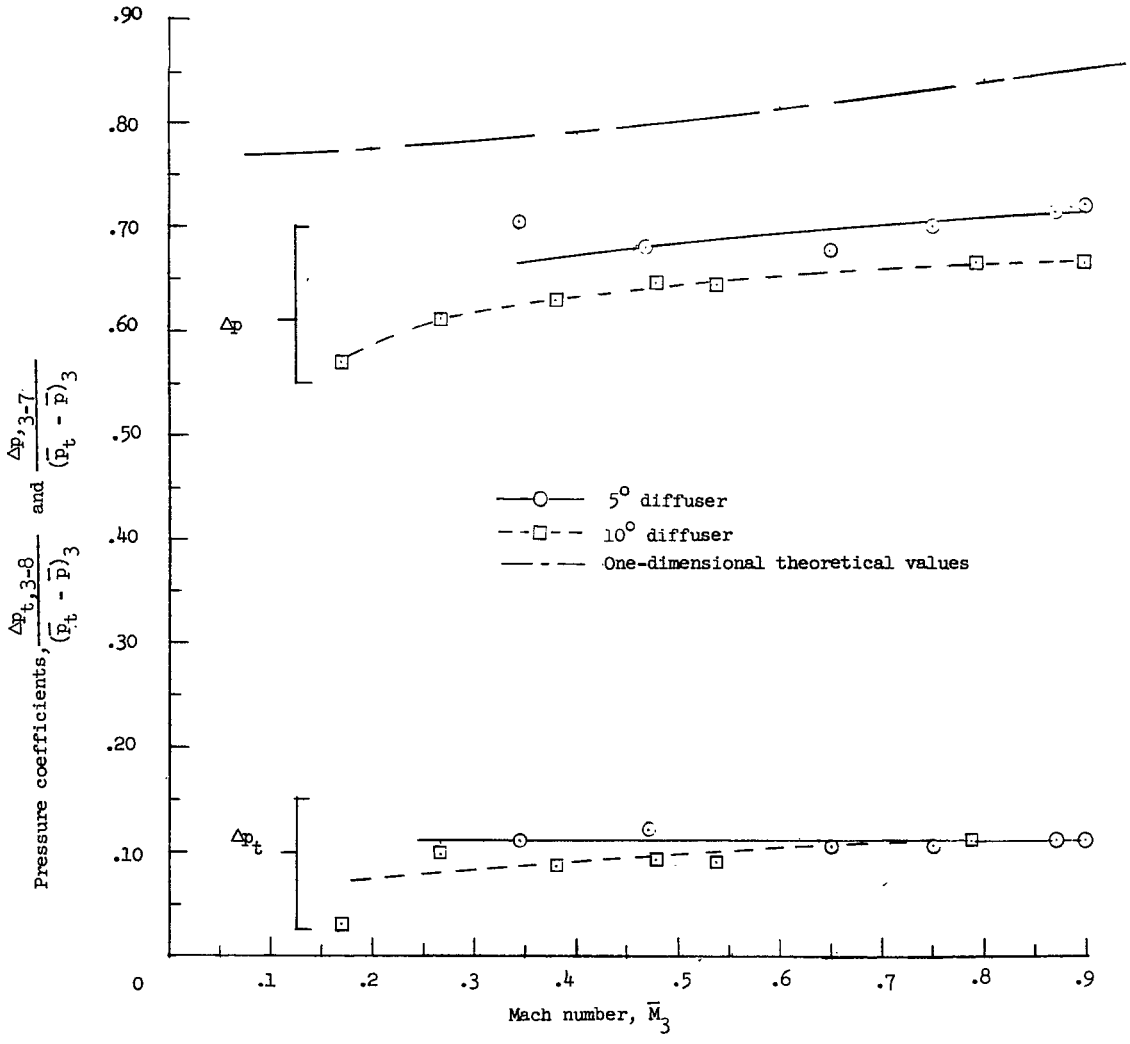

Figure 7.- Variation of pressure coefficients with Mach number. Configuration I; subsonic-flow condition.

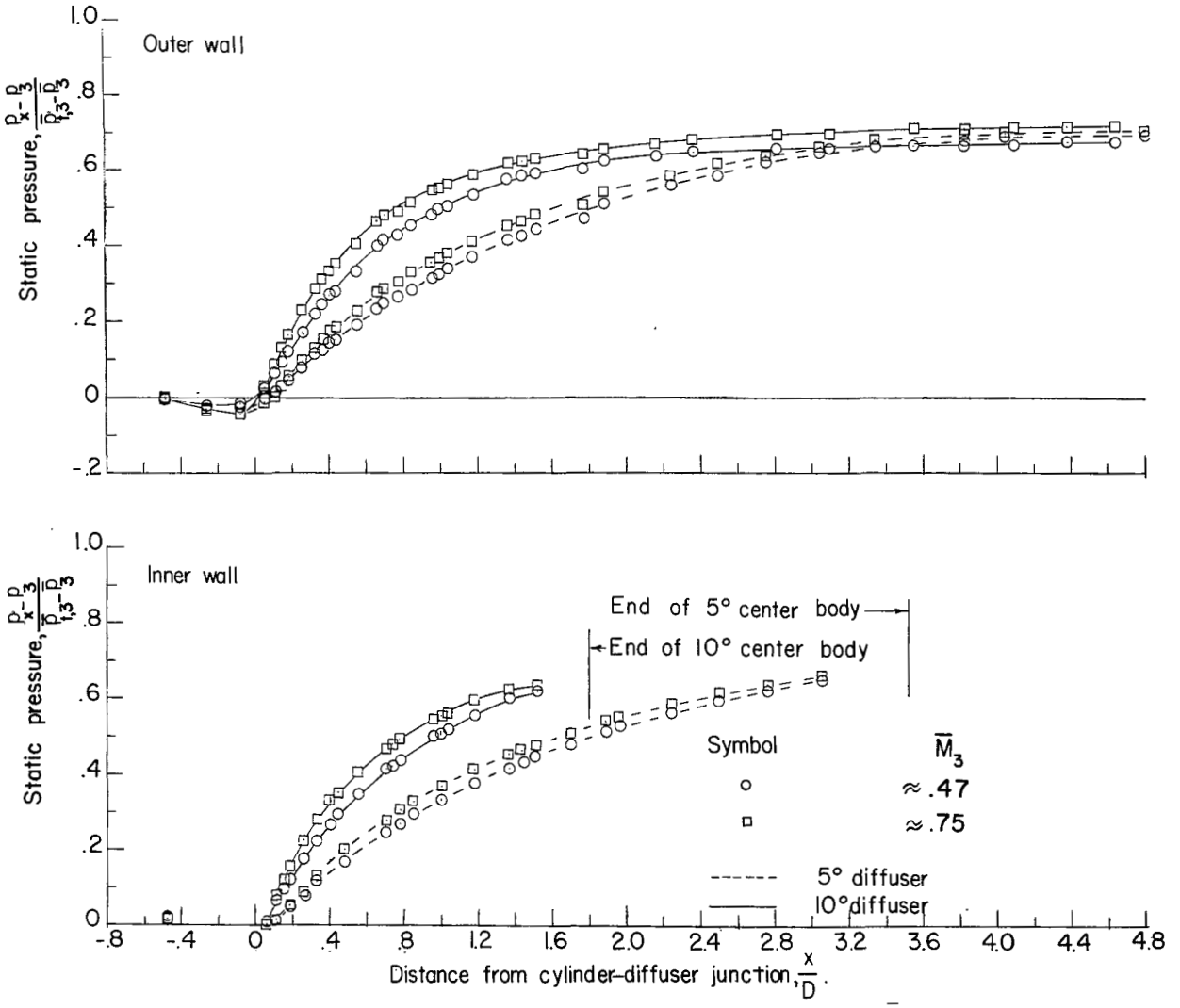

Figure 8.- Longitudinal wall static-pressure distributions for configuration I. Subsonic-flow condition.

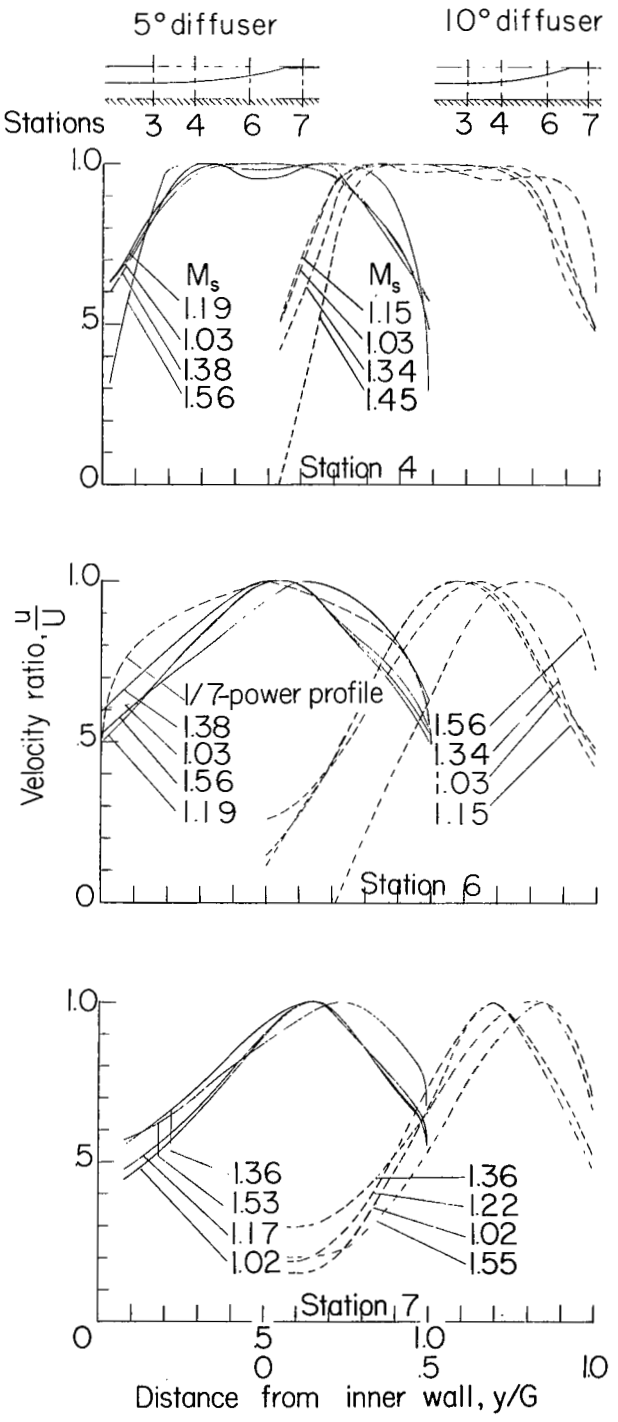

Figure 9.- Velocity distributions for configuration I. Supersonic-flow condition.

[redacted]

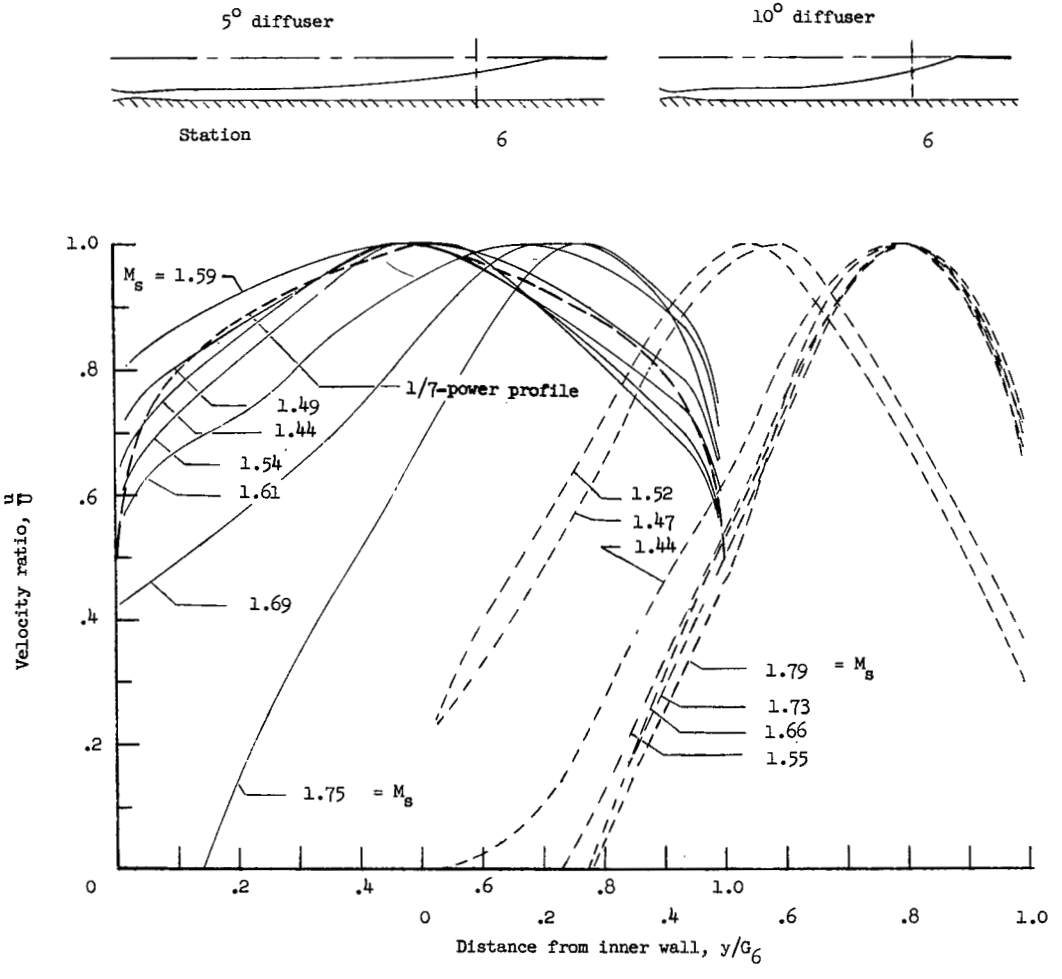

(a) Velocity distributions.

Figure 10.- Velocity distributions and total-pressure distortions at station 6. Configuration II.

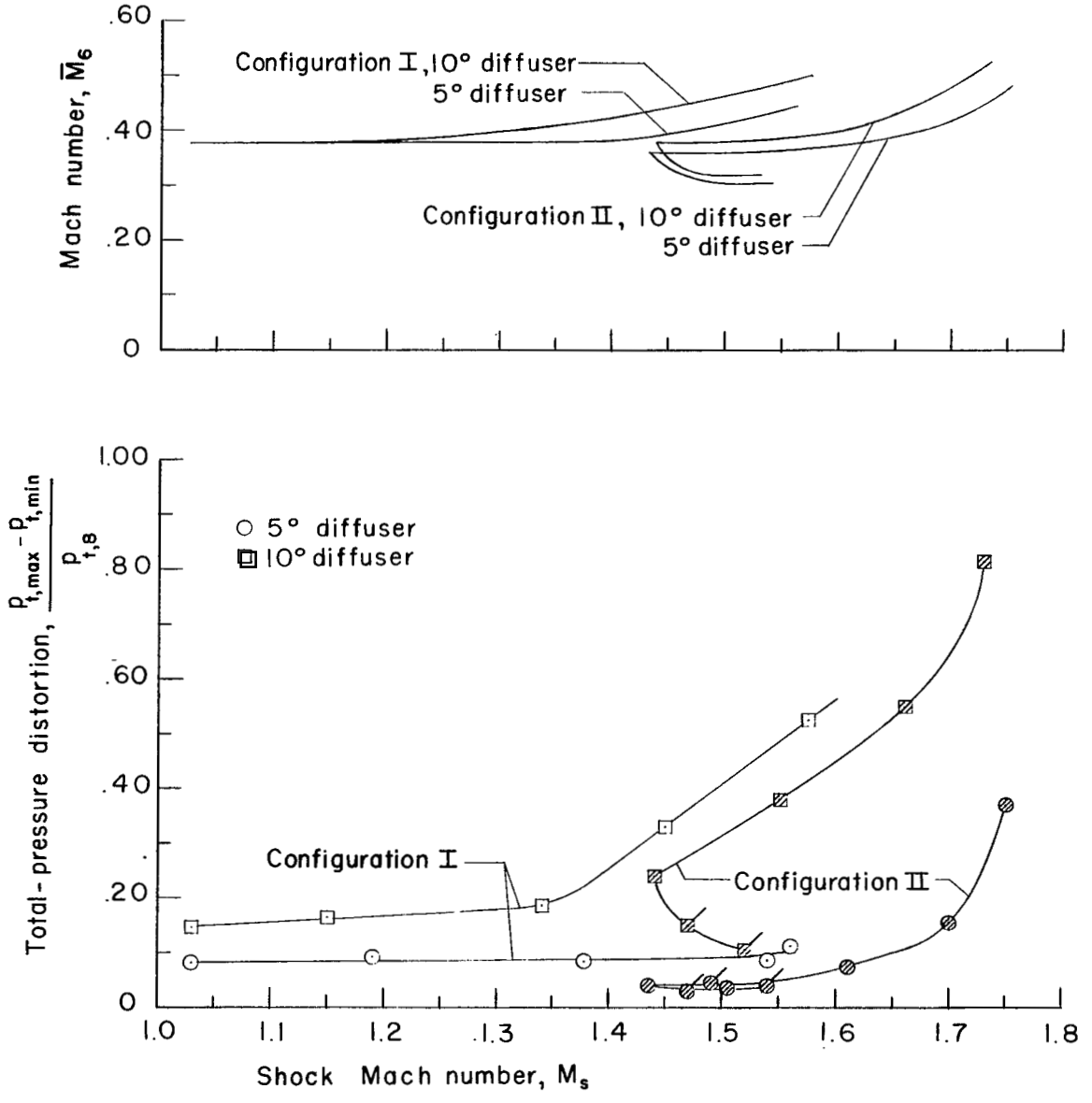

(b) Total-pressure distortion. Tabs indicate shock located in constant-area duct upstream of diffuser.

Figure 10.- Concluded.

[redacted]

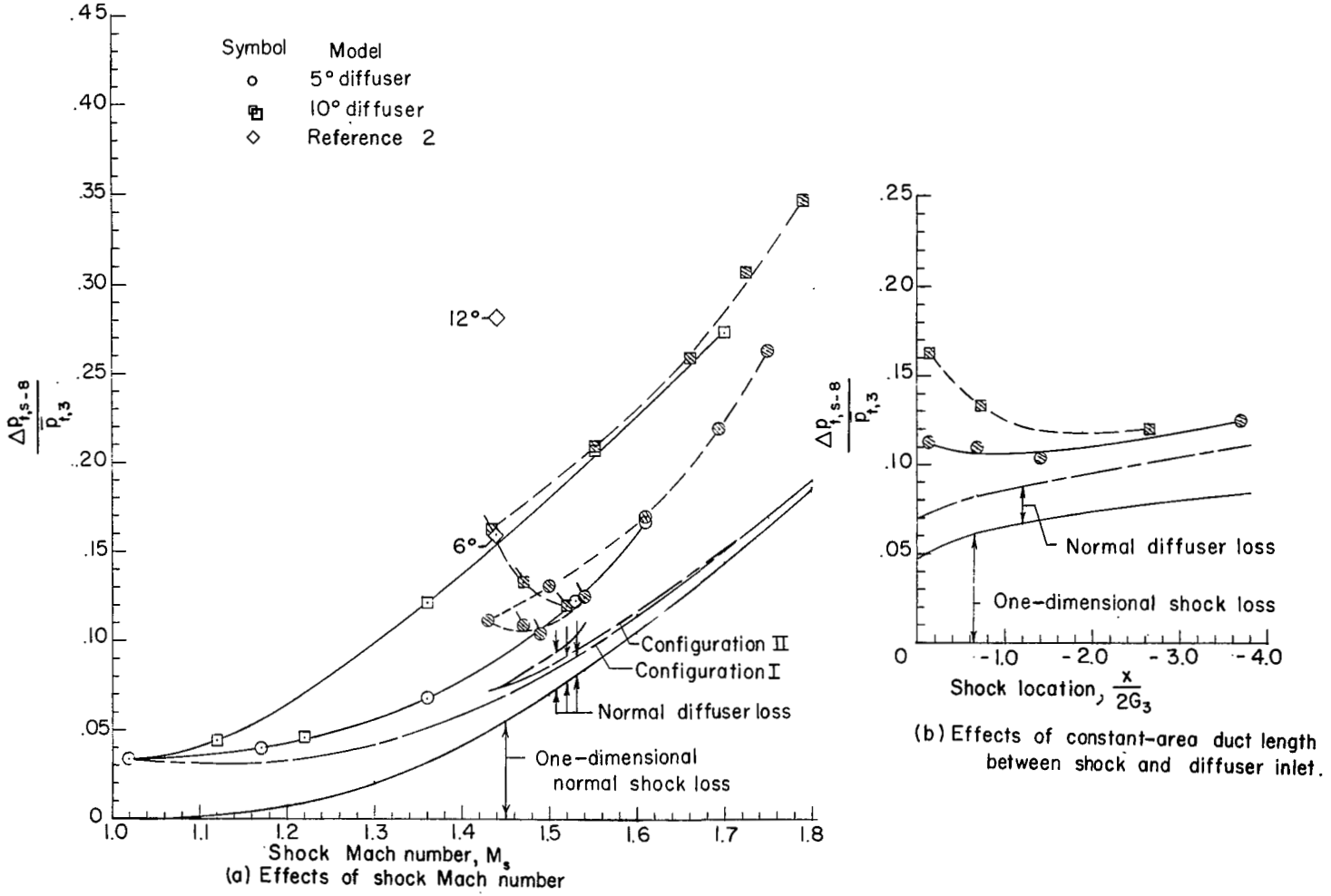

Figure 11.- Variation in diffuser total-pressure loss with shock Mach number and length of constant-area duct between shock and diffuser entrance. Shaded symbols indicate configuration II; tabs indicate shock located in constant-area section.

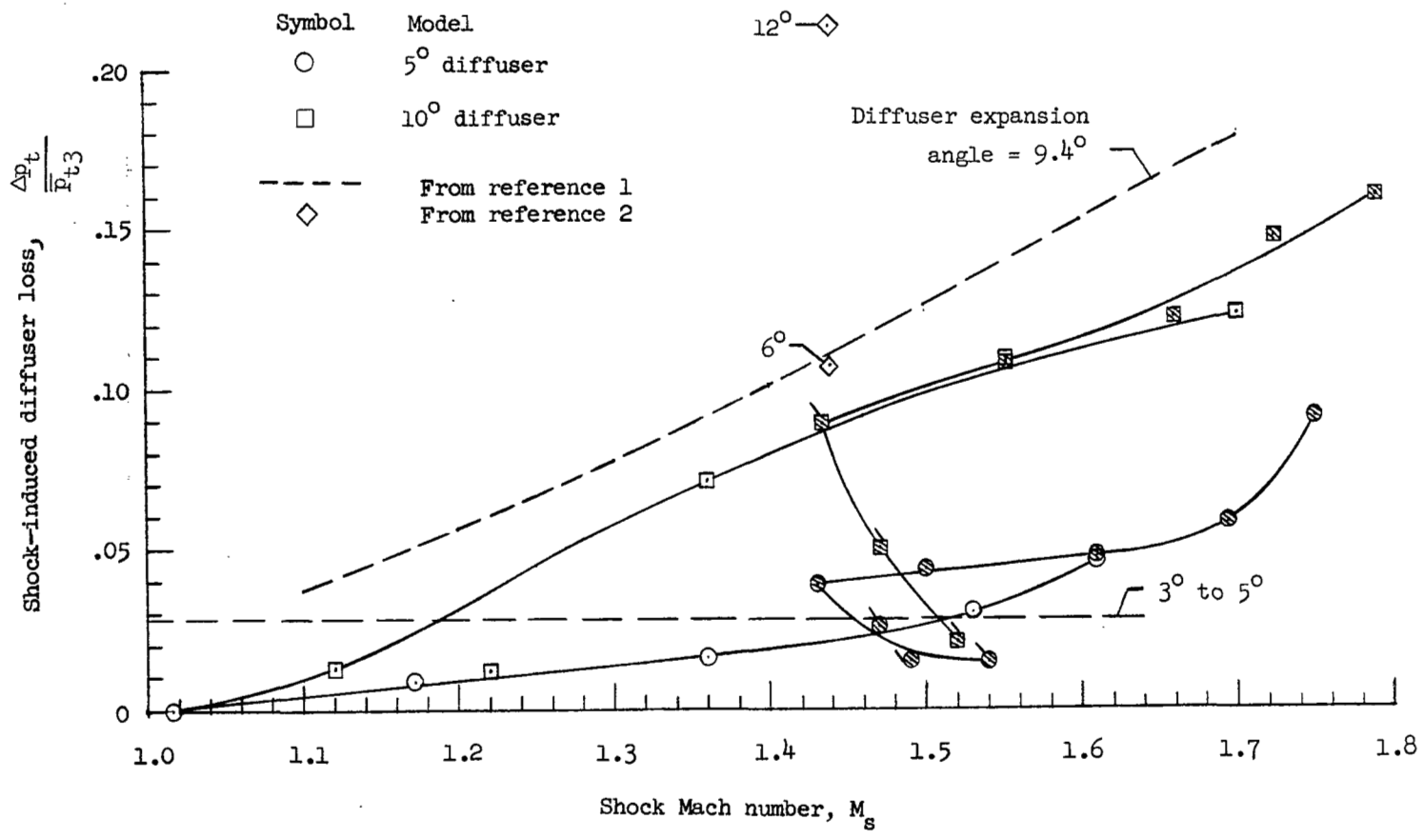

Figure 12.- Variation of shock-induced diffuser loss with shock Mach number. Shaded symbols indicate configuration II; tabs indicate shock located in constant-area section.

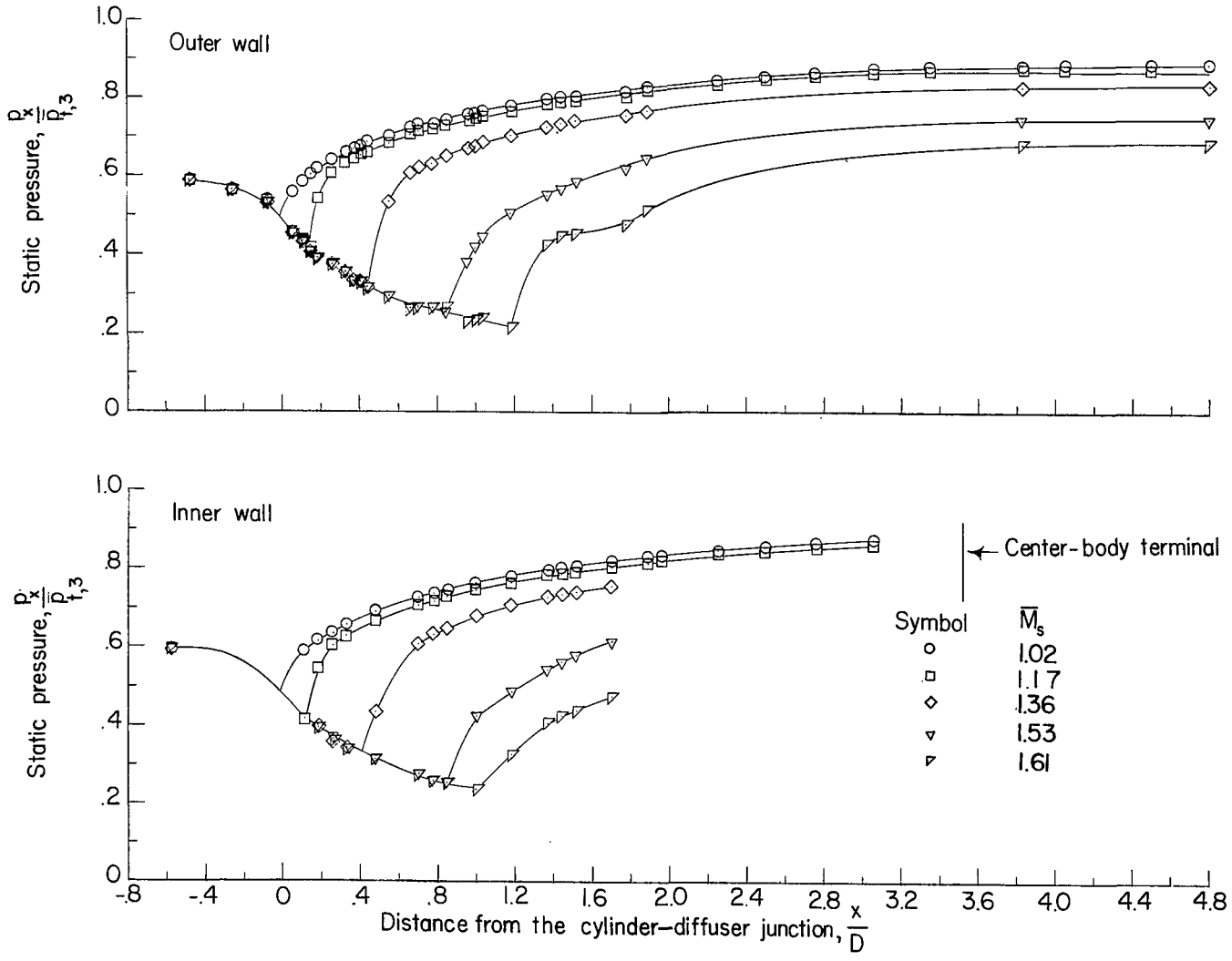

Figure 13.- Longitudinal wall static-pressure distributions for several shock locations. Configuration I; 5° diffuser.

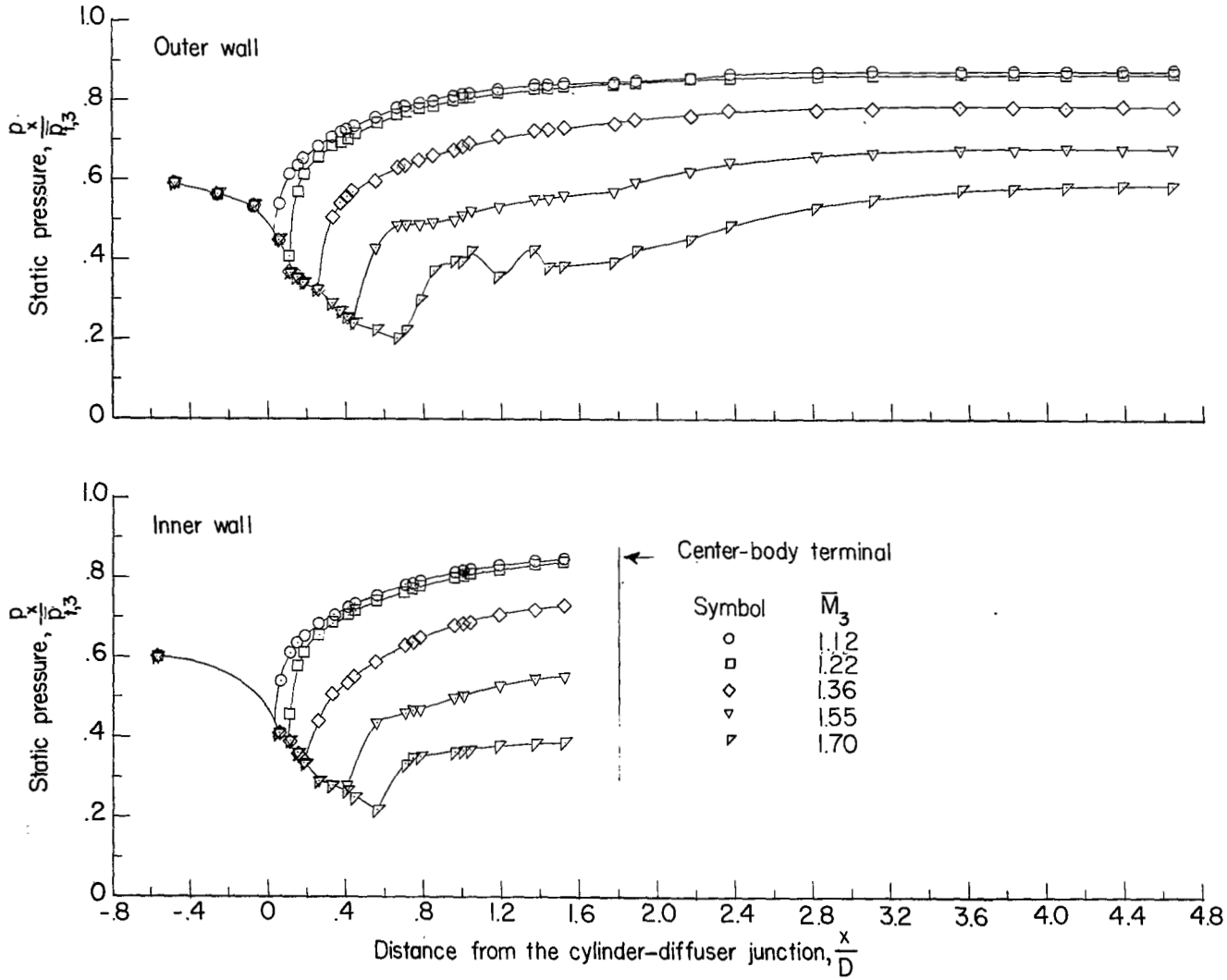

Figure 14.- Longitudinal wall static-pressure distributions for several shock locations. Configuration I; 10° diffuser.

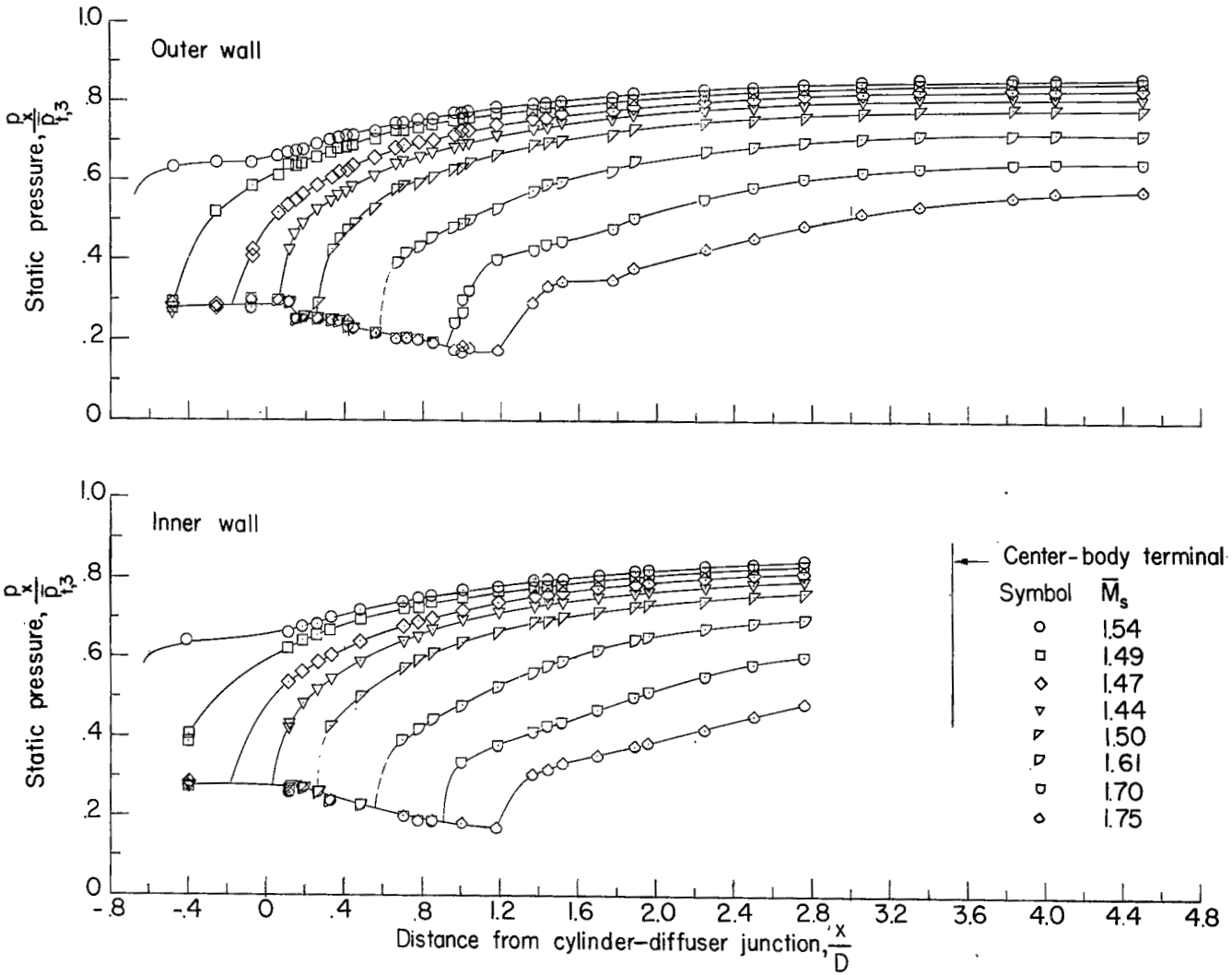

Figure 15.- Longitudinal wall static-pressure distributions for several shock locations. Configuration II; 5° diffuser.

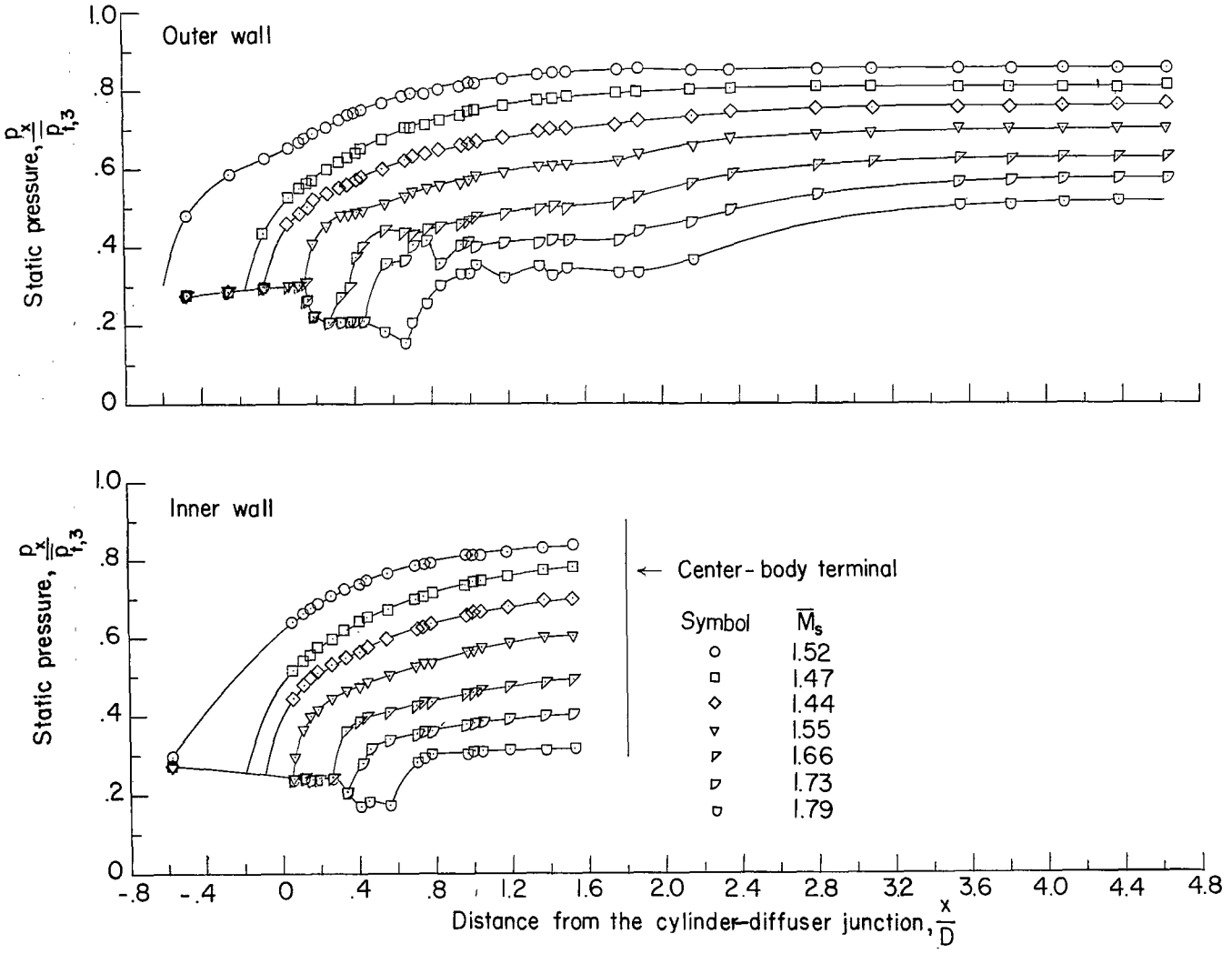

Figure 16.- Longitudinal wall static-pressure distributions for several shock locations. Configuration II; 10° diffuser.

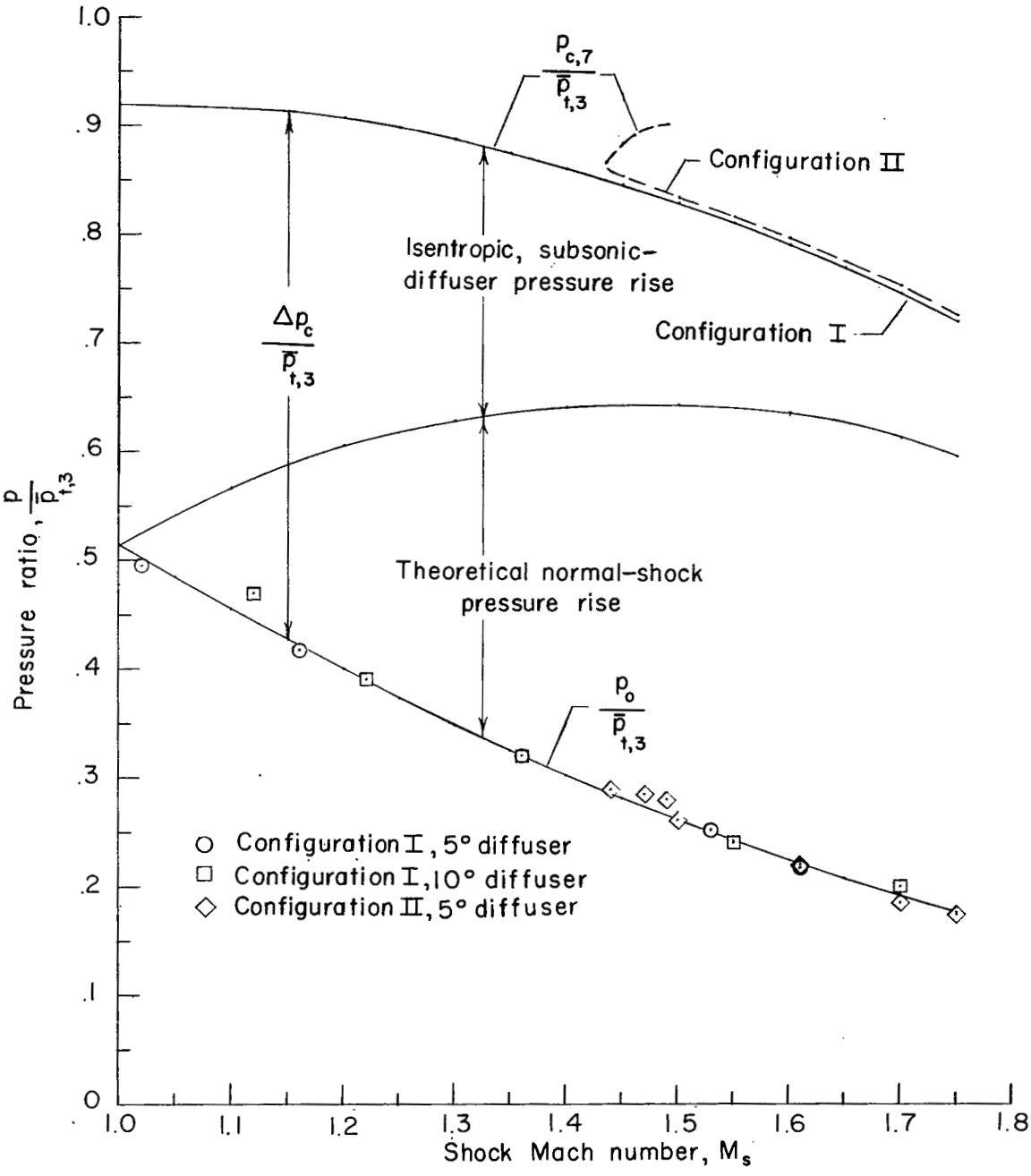

Figure 17.- Variation with shock Mach number of diffuser static-pressure rise due to shock waves and isentropic diffusion.

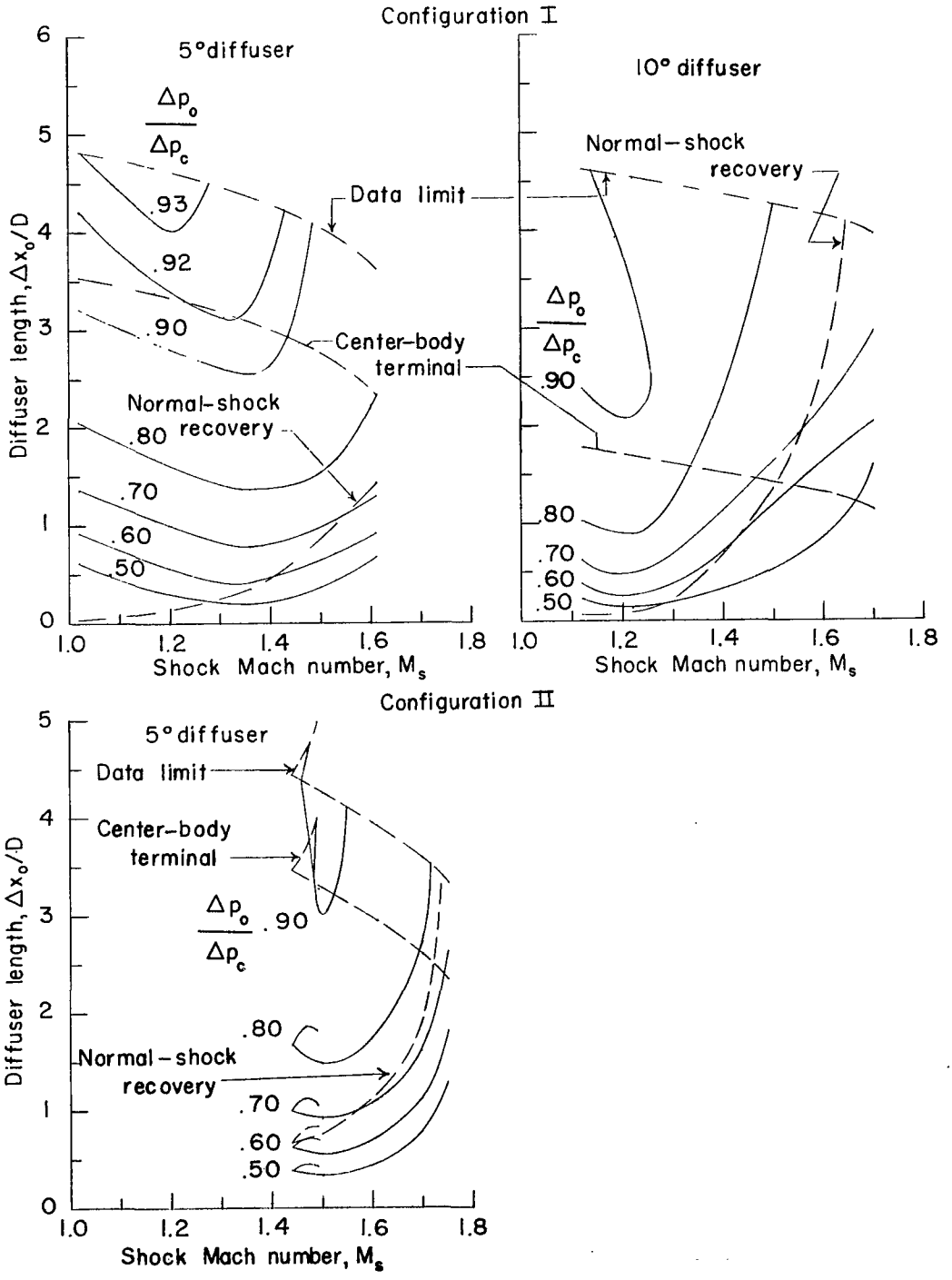

Figure 18.- Diffuser lengths required to recover the theoretical static-pressure rise.

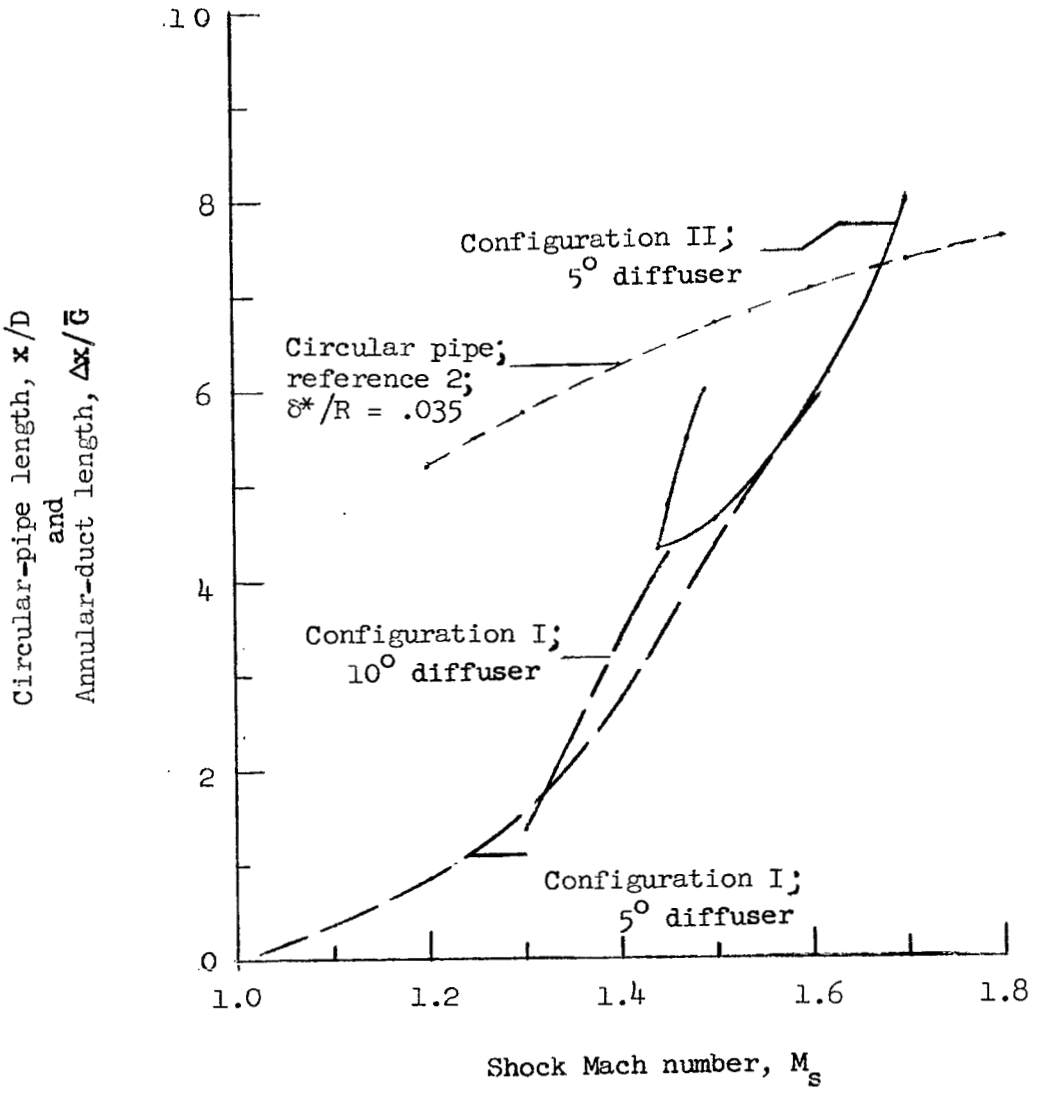

Figure 19.- Duct length required to recover normal-shock pressure rise.

NACA - Langley Field, Va.

[redacted]

[redacted]